RESEARCH ARTICLE

Molecular Mechanism of Flocculation Self-Recognition in Yeast and Its Role in Mating and Survival

Katty V. Y. Goossens,[a] Francesco S. Ielasi,[a] Intawat Nookaew,[b]* Ingeborg Stals,[c,d] Livan Alonso-Sarduy,[e] Luk Daenen,[f] Sebastiaan E. Van Mulders,[f] Catherine Stassen,[d] Rudy G. E. van Eijsden,[g] Verena Siewers,[b] Freddy R. Delvaux,[f] Sandor Kasas,[e] Jens Nielsen,[b] Bart Devreese,[d] Ronnie G. Willaert[a]

Department of Bioengineering Sciences, Structural Biology Research Center, Vrije Universiteit Brussel, Brussels, Belgium[a]; Department of Chemical and Biological Engineering, Chalmers University of Technology, Gothenburg, Sweden[b]; Faculty of Applied Engineering Sciences, Hogeschool Gent, Ghent, Belgium[c]; Department Biochemistry and Microbiology, Laboratory for Protein Biochemistry and Biomolecular Engineering, Ghent University, Ghent, Belgium[d]; Laboratoire de Physique de la Matière Vivante, École Polytechnique Fédérale de Lausanne (EPFL), Lausanne, Switzerland[e]; Centre for Malting and Brewing Sciences, KU Leuven, Heverlee, Belgium[f]; VIB Nucleomics Core, VIB, Leuven, Belgium[g]

* Present address: Intawat Nookaew, Comparative Genomics Group, Biosciences Division, Oak Ridge National Laboratory, Oak Ridge, Tennessee, USA.

K.V.Y.G. and F.S.I. contributed equally to this article.

ABSTRACT **We studied the flocculation mechanism at the molecular level by determining the atomic structures of N-Flo1p and N-Lg-Flo1p in complex with their ligands. We show that they have similar ligand binding mechanisms but distinct carbohydrate specificities and affinities, which are determined by the compactness of the binding site. We characterized the glycans of Flo1p and their role in this binding process and demonstrate that glycan-glycan interactions significantly contribute to the cell-cell adhesion mechanism. Therefore, the extended flocculation mechanism is based on the self-interaction of Flo proteins and this interaction is established in two stages, involving both glycan-glycan and protein-glycan interactions. The crucial role of calcium in both types of interaction was demonstrated: Ca^{2+} takes part in the binding of the carbohydrate to the protein, and the glycans aggregate only in the presence of Ca^{2+}. These results unify the generally accepted lectin hypothesis with the historically first-proposed "Ca^{2+}-bridge" hypothesis. Additionally, a new role of cell flocculation is demonstrated; i.e., flocculation is linked to cell conjugation and mating, and survival chances consequently increase significantly by spore formation and by introduction of genetic variability. The role of Flo1p in mating was demonstrated by showing that mating efficiency is increased when cells flocculate and by differential transcriptome analysis of flocculating versus nonflocculating cells in a low-shear environment (microgravity). The results show that a multicellular clump (floc) provides a uniquely organized multicellular ultrastructure that provides a suitable microenvironment to induce and perform cell conjugation and mating.**

IMPORTANCE **Yeast cells can form multicellular clumps under adverse growth conditions that protect cells from harsh environmental stresses. The floc formation is based on the self-interaction of Flo proteins via an N-terminal PA14 lectin domain. We have focused on the flocculation mechanism and its role. We found that carbohydrate specificity and affinity are determined by the accessibility of the binding site of the Flo proteins where the external loops in the ligand-binding domains are involved in glycan recognition specificity. We demonstrated that, in addition to the Flo lectin-glycan interaction, glycan-glycan interactions also contribute significantly to cell-cell recognition and interaction. Additionally, we show that flocculation provides a uniquely organized multicellular ultrastructure that is suitable to induce and accomplish cell mating. Therefore, flocculation is an important mechanism to enhance long-term yeast survival.**

Received 21 March 2015 **Accepted** 24 March 2015 **Published** 14 April 2015

Citation Goossens KVY, Ielasi FS, Nookaew I, Stals I, Alonso-Sarduy L, Daenen L, Van Mulders SE, Stassen C, van Eijsden RGE, Siewers V, Delvaux FR, Kasas S, Nielsen J, Devreese B, Willaert RG. 2015. Molecular mechanism of flocculation self-recognition in yeast and its role in mating and survival. mBio 6(2):e00427-15. doi:10.1128/mBio.00427-15.

Editor Sang Yup Lee, Korea Advanced Institute of Science and Technology

Address correspondence to Ronnie G. Willaert, Ronnie.Willaert@vub.ac.be.

Many fungi contain a family of cell wall glycoproteins called "adhesins" that confer unique adhesion properties (1–3). These proteins are required for the interactions of fungal cells with each other in processes such as flocculation and filamentation (1, 2, 4). The members of the Flo adhesin protein family in *Saccharomyces cerevisiae* can be subdivided into two groups (2). The members of the first group of proteins are encoded by genes, including *FLO1*, *FLO5*, *FLO9*, and *FLO10*, which share considerable sequence homology. The gene products of *FLO1*, *FLO5*, *FLO9*, and—to a lesser extent—*FLO10* (5) promote cell-cell adhesion and contribute to the formation of multicellular clumps (flocs), which sediment out of solution and are therefore called flocculins (6). Flo1p leads to a strong flocculation phenotype and is considered the most dominant adhesion protein (5, 7, 8). The members of the second group of the Flo family, including Flo11p, Fig2p, and Aga1p, have a domain structure similar to that of the first, but with

quite unrelated amino acid sequences. Flo11p also promotes cell-cell adhesion, but does this only weakly (5). Flo11p is mainly required for diploid pseudohyphal formation, haploid invasive growth (4, 9), and biofilm formation (10, 11). N-Flo11p does not bind mannose, which is in contrast to the other Flo proteins. However, N-Flo11p can interact with N-Flo11p (homophilic adhesion ability), explaining the weak-flocculation characteristic (12, 13).

Flocculins consist structurally of three domains and are anchored in the cell wall by a glycosylphosphatidylinositol (GPI) anchor (14, 15). The Flo proteins interact with other yeast cells through their N-terminal mannose-binding domain (7, 16). The N-terminal carbohydrate-binding domains of the Flo1 flocculins from both *S. cerevisiae* (N-Flo1p) and *S. pastorianus* (N-Lg-Flo1p) belong to the PA14 domain family (Pfam entry PF07691) (17). The presence of a Ca^{2+}-dependent carbohydrate-binding site is a common element in the PA14 domain family (18, 19). The structure of N-Flo1p, which shares with the correspondent domain of Flo5p (20) more than 90% of its amino acid sequence, had not been solved until the present. The structure of the apo form of N-Lg-Flo1p has been recently solved (21), but the adapted protein structure upon carbohydrate ligand binding had not yet been elucidated. Like most of the cell wall proteins, the N-terminal domain of Flo1p is heavily N- and O-glycosylated (22, 23), but the exact glycan profile and the role of these glycans in the molecular binding mechanism are not yet known.

Two major cases of cell-cell adhesion events are flocculation and mating. Both events enhance the survival of yeast cells. Mating between cells of opposite mating types enables genetic recombination, while flocculation is recognized as a way for cells in solution to escape from harsh conditions by sedimentation. Flocculation also protects the inner cells of the floc from multiple stresses, including antimicrobials and ethanol (24).

In this study, the atomic structures of the N-terminal domains of Flo1p and Lg-Flo1p in complex with calcium and the ligand carbohydrates were determined by X-ray crystallography. A thorough investigation of the glycans present on the protein was done, showing that N-Flo1p is expressed in two populations due to the occurrence of 2 glycoforms. Furthermore, the homophilic N-Flo1p–N-Flo1p interaction occurring through lectin-carbohydrate binding was characterized at the molecular level, and the contribution of the glycan-glycan interaction to N-Flo1p self-binding was investigated by atomic force microscopy (AFM) imaging and force spectroscopy. These results refine and extend the flocculation mechanism at the molecular level by elucidating the role played by glycosylated flocculins and glycans in cell-cell adhesion. Moreover, liquid growth experiments in a low-shear microgravity (μg) environment revealed that flocculation is linked to mating (and sporulation), since flocculation provides an organized multicellular ultrastructure with in-floc conditions suitable for conjugation and mating. This was confirmed experimentally by mating assays. These results extend understanding of the role of cell flocculation in cell survival under adverse conditions by enhancing the mating efficiency of cells.

RESULTS

N-Flo1p and N-Lg-Flo1p share significant structure identity with N-Flo5p but establish additional interactions with the ligand through the L3 loop. The overall structure of apo-N-Flo1p (Fig. 1A; see also Fig. S1 in the supplemental material) (PDB code 4LHL) is very similar to the crystal structure of apo-N-Flo5p (PDB code 2XJQ): the two adhesion domains share 95% sequence identity and can be superposed with a C_α root mean square deviation (RMSD) of 0.31 Å over 241 residues (Fig. 1B). On the other hand, the superposition of the apo-N-Lg-Flo1p (PDB code 4GQ7) and apo-N-Flo1p structures, which are identical for 74% of their sequences, gives a C_α RMSD of 0.59 Å over 213 residues (Fig. 1B).

N-Flo1p is characterized by the presence of a Flo subdomain (N84 to M110), i.e., the Flo1 subdomain (Fig. 1A), which is situated near the binding site. It is stabilized by two disulfide bonds and plays a role in binding specificity for mannosides (20). It is absent in the structures of N-Lg-Flo1p (21) and N-Epa1p (25), where it is replaced by the L2 loop (G84-N135 in N-Lg-Flo1p). Loop L3 (amino acids [aa] 193 to 204) is present in N-Flo1p and N-Lg-Flo1p, as well as in N-Flo5p and N-Epa1p (25), and is involved in carbohydrate ligand binding. Most likely, residue 202 (P in N-Flo1p and D in N-Flo5p) determines the flexibility of this loop (Fig. 1B). The complete modeling of L3 in the apo form of N-Flo1p was not possible since the electron density for residues W196 to G198 and part of S199 was missing, which was most probably due to the high flexibility of this loop. The corresponding L3 loop is also quite flexible in apo-N-Lg-Flo1p and is positioned closer to the binding site than in N-Flo1p (Fig. 1B).

The interaction geometry of the N-Flo1p binding pocket (Fig. 1C) (PDB code 4LHN) closely matches that of the N-Flo5p-mannose complex (20). Ca^{2+} is coordinated on carbohydrate binding loop 1 (CBL1) (residues 157 to 161) by *cis* peptides D160 and D161 and on CBL2 (residues 225 to 228) by the N224 side chain and by the main chain carbonyl groups of V226 and W228. Residues D160, D161, and N224 are strongly conserved in the Flo and Epa adhesin families due to their importance for metal docking (20, 26). The coordination shell is completed upon binding of mannose by the 3′- and 4′-hydroxyl groups at a distance of 2.6 Å, which creates a distorted pentagonal bipyramidal geometry. Mannose establishes hydrogen bonds between its 3′- and 4′-hydroxyl groups and the aspartates of the *cis* peptide and between the oxygen in position 2′ and Q98. The side chain of Q98 in the Flo1 subdomain is responsible for the discrimination between the axial mannose and equatorial glucose hydroxyls on C2. In contrast to N-Flo5p, where there is no significant difference in the positions of the L3 loop between the bound state and unbound state (20), in N-Flo1p, remarkably, this loop approaches the CBL1 loop upon carbohydrate binding, especially where it functions as a lid for the active site. P202 in the dipeptide consisting of P201 and P202 seems to constrain L3 to a single conformation, while two conformations were proposed for N-Flo5p, even in the bound state (20). Under these conditions, the side chain of K194 in N-Flo1p can readily interact with the mannose 6′-OH and the axial 2′-OH, and W196 further stabilizes the binding by means of dispersion forces.

Imitating the Ca^{2+}-dependent carbohydrate recognition of N-Flo1p and N-Flo5p, N-Lg-Flo1p in complex with α-1,2-mannobiose (Fig. 1D) (PDB code 4LHK) coordinates the Ca^{2+} cation through the side chains of highly conserved D133, D134, and N197 (on CBL1) and the main chain of the variable K199 and L201 (on CBL2). The Flo1 subdomain is absent here, and so are any equivalents of N-Flo5p residues Q98 and Q117. The latter is involved in a hydrogen bond with the 3′-hydroxyl group on the reducing moiety of α-1,2-mannobiose (20). The L2 loop in N-Lg-Flo1p replaces the flocculin subdomain in N-Flo1p and establishes hydrophobic interactions with the disaccharide through the

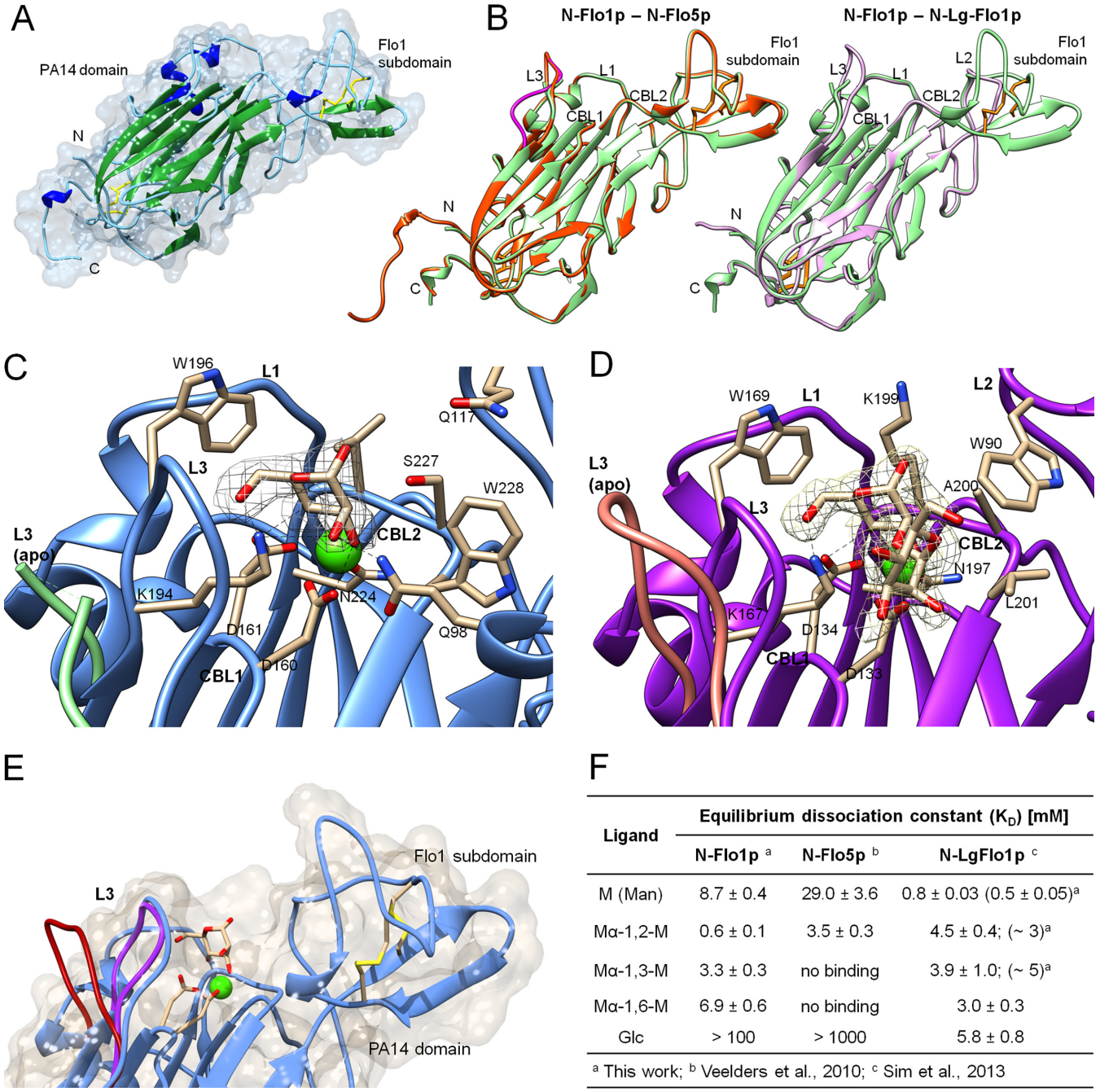

Ligand	Equilibrium dissociation constant (K_D) [mM]		
	N-Flo1p [a]	N-Flo5p [b]	N-LgFlo1p [c]
M (Man)	8.7 ± 0.4	29.0 ± 3.6	0.8 ± 0.03 (0.5 ± 0.05)[a]
Mα-1,2-M	0.6 ± 0.1	3.5 ± 0.3	4.5 ± 0.4; (~ 3)[a]
Mα-1,3-M	3.3 ± 0.3	no binding	3.9 ± 1.0; (~ 5)[a]
Mα-1,6-M	6.9 ± 0.6	no binding	3.0 ± 0.3
Glc	> 100	> 1000	5.8 ± 0.8

[a] This work; [b] Veelders et al., 2010; [c] Sim et al., 2013

FIG 1 Structures of N-Flo1p and N-Lg-Flo1p and their interaction with carbohydrate ligands. (A) Structure and surface shape of the apo form of the Flo1p N-terminal carbohydrate-binding domain (PDB code 4LHL). The β-sheets of the PA14-like domain kernel are depicted in green, α-helices in dark blue, and disulfide bonds in yellow (see also Fig. S1 in the supplemental material). (B) Comparison of the Flo apo structures: superpositions of the N-terminal domain of Flo1p (green ribbons, PDB code 4LHL) on N-Flo5p (orange ribbon, PDB code 2XJQ) (left subpanel), and N-Lg-Flo1p (lilac ribbon, PDB code 4GQ7) (right subpanel). The main structural features of the flocculin domains are indicated. In all structures, disulfide bonds are indicated in yellow. In the left subpanel, the alternate conformation of N-Flo5p L3 loop is indicated in magenta. (C) The N-Flo1p (PDB code 4LHN) carbohydrate-binding site in complex with calcium and mannose. The side chains of the main residues participating in ligand binding are shown and labeled. Ca^{2+} is depicted as a green sphere. Mesh surfaces around ligands represent their electron density from the respective omit maps, generated with SFCHECK (131) (contour level: 1 σ for mannose, 0.8 σ for mannobiose). The position of the L3 loop for the unbound state is indicated in light green; the unbound-bound shift has an RMSD of 4.66, region I193 to N203 (see also Fig. S1). (D) The N-Lg-Flo1p (PDB code 4LHK) carbohydrate-binding site, in complex with calcium and α-1,2-mannobiose. The position of the L3 loop for the unbound state is indicated in salmon; the unbound-bound shift has an RMSD of 3.78, region I166 to D176 (see also Fig. S1). (E) Partial view of the NFlo1p binding pocket (light blue ribbon/surface) in complex with calcium mannose. Conformations of the L3 loop from N-Lg-Flo1p (purple) and N-Flo5p (crimson; from PDB entry 2XJP) bound states are also shown for comparison. (F) *In vitro* binding affinities of NFlo1p, N-Flo5p, and N-Lg-Flo1p for monosaccharides and disaccharides, measured by fluorescence titrations. The work by Veelders et al. may be found in reference 20; the work by Sim et al. may be found in reference 21.

indole ring of W90. The K199, A200, and L201 residues on the CBL2 loop also contribute by creating a hydrophobic environment around the ligand, which is then further "sealed" on one side by L3. As in N-Flo1p, L3 in N-Lg-Flo1p is much closer to the binding site than in N-Flo5p (Fig. 1E), and it is locked in one conformation. From this loop, the side chain of K167 acts as a hydrogen-bond donor with the 6′-OH on the reducing hexose moiety, and residue W169 is again involved in the binding network, mainly via hydrophobic interactions.

N-Flo1p recognizes mannose and mannobioses with higher affinity than N-Flo5p and is more specific than N-Lg-Flo1p for mannose oligosaccharides. The nonglycosylated N-Flo1p and N-Lg-Flo1p constructs were used in fluorescence titration experiments to determine the equilibrium constants for mannosides (Fig. 1F). The affinity of N-Flo1p for D-mannose was found to be in the low-millimolar range (K_D [equilibrium dissociation constant] of 8.7 ± 0.43 mM), which is three times higher than the reported value for N-Flo5p (29.3 ± 3.6 mM) (20). A higher affinity was found for α-1,2-mannobiose (630 ± 50 μM), confirming the trend observed for N-Flo5p, with a 10-fold difference in binding between the mono- and disaccharides. Surprisingly, N-Flo1p was also able to recognize the α-1,3- and α-1,6-linked mannobiose molecules (K_D of 3.3 ± 0.34 mM and 6.9 ± 0.64 mM, respectively). No binding of these two disaccharides was detected for N-Flo5p (20). As expected, both Flo proteins interact very weakly with glucose. Concerning N-Lg-Flo1p, our fluorescence measurements on a few ligands basically corroborated data recently published by others (21). The K_D values for the N-Lg-Flo1p construct from the CBS1513 strain are comparable to the value for the CG2164 strain and fall within either the high micromolar range (D-mannose) or the millimolar range (mannobioses).

Both N-Flo1p populations contain three N-glycosylation sites with core as well as hyperglycosylated type N-glycans and three O-glycosylation sites with two mannoses per site. N-Flo1p is both O- and N-glycosylated and is expressed in *S. cerevisiae* in two populations, distinguished by their apparent molecular masses of around 36 kDa and 100 kDa (22). From the oligosaccharide analysis of the N-glycans (see Fig. S3 in the supplemental material), it is clear that both N-Flo1p populations contain both short Man8–14GlcNAc oligosaccharides (core type) and large Man>50GlcNAc N-glycans (hyperglycosylated type) but in different ratios: 2 oligomannoses and 1 hyperglycosylated structure for the 36-kDa N-Flo1p population and 1 oligomannose and 2 hyperglycosylated structures for the 100-kDa N-Flo1p population. Thus, the three N-glycosylation sites (N135, N187, and N262) that were predicted by the NetNGlyc online server (27) are glycosylated.

Electrospray ionization-mass spectrometry (ESI-MS) was performed on both populations of N-deglycosylated N-Flo1p, and exactly identical profiles were observed (see Fig. S6A and B in ths supplemental material), which implies that they carry equal amounts of O-glycans. Based on the molecular mass of the N-deglycosylated proteins detected in the spectra (29,317 Da), 5 or 6 mannoses are present on the N-terminal domain of Flo1p, taking into account the remaining GlcNAc residues after EndoH (endo-β-*N*-acetylglucosaminidase H) treatment. To estimate the amount of O-glycosylation sites, the mass of the N- and O-deglycosylated N-Flo1 protein was analyzed using ESI-MS (see Fig. S6C), giving a mass of 28,868 Da, from which it is calculated that 3 O-glycosylation sites are present. These results demonstrate that at least two O-glycosylation sites contain 2 mannose residues and that the third site has 1 or 2 mannoses.

N-Flo1p shows a homophilic interaction mediated by its N-glycans. The binding of the N-Flo1p to the glycans of other N-Flo1 proteins was determined qualitatively by surface plasmon resonance (SPR) (Fig. 2A). The concentration-dependent increase in signal indicates that N-Flo1p is able to bind to N-Flo1p. The affinity of the interaction was estimated in the micromolar range (7 μM). When N-deglycosylated N-Flo1p was injected over the chip with immobilized N-deglycosylated N-Flo1p, almost no binding was observed.

Force spectroscopy was used to further analyze this interaction on the single-molecule level (Fig. 2B to D, left subpanels; see also Fig. S2 in the supplemental material). In the presence of Ca^{2+}, unbinding events were detected in the range between 100 and 600 pN (Fig. 2B), and with an event peak of around 300 pN. An evident decrease in the number of main peak events is observed when mannose is added (Fig. 2C). A situation completely devoid of unbinding statistics could be reached when both mannose and EDTA were present in solution (Fig. 2D), confirming the activity of EDTA and mannose as inhibitors for the N-Flo1p–glycan binding.

N-Flo1p glycans aggregate in the presence of Ca^{2+}. The role of the N-Flo1p glycans themselves in the homophilic adhesion property of N-Flo1p was examined using AFM and force spectroscopy by analyzing force-distance scatter plots (Fig. 2B to D, right subpanels). Interactions between glycosylated N-Flo1p molecules in the presence of Ca^{2+} covered a wide range of distances, up to approximately 350 nm in the distance ramp (Fig. 2B). During inhibition with mannose, fewer unbinding events took place closer to the surface (between 100 and 200 nm), but a significant number of binding ruptures were still detected beyond 200 nm (Fig. 2C), most likely independently from the flocculin mannose-specific activity and attributable to glycan-glycan interactions. As a result of the addition of EDTA as a second binding inhibitor, these longer-distance events disappeared almost completely, and only a few interactions (probably aspecific ones) were observed (Fig. 2D). Therefore, mannose acts as a specific inhibitor for the protein-carbohydrate interactions, which are rather homogeneous in terms of strength and distance, while the chelating agent totally disrupts the heterogeneity of the interactions, affecting not only the mannose-sensitive protein-carbohydrate-binding events but also long-range events (which appear to be Ca^{2+} sensitive but mannose insensitive). The long-range events are possibly due to strongly ionic, Ca^{2+}-mediated carbohydrate-carbohydrate interactions, most probably due to mannosyl-phosphate groups present on the N-linked glycans. This phenomenon was further assessed by visualizing the N-glycans released from the 100-kDa population of N-Flo1p with AFM. In the presence of Ca^{2+}, the glycans aggregated (Fig. 3A and C), and in the absence of Ca^{2+}, the glycans did not aggregate and adopted a more globular conformation (Fig. 3B).

Cell flocculation enhances mating efficiency. The effect of Flo8p activation and Flo1p overexpression on cell-cell interaction processes was investigated by transcriptome analysis. The differential gene expression derived from the comparison of BY4742:: *FLO8* and *FLO1* overexpression strains to the nonflocculating BY4742 wild-type (WT) strain under 1-*g* and low-shear (*μg*) growth conditions is summarized as a Venn's diagram in Fig. 4A. The growth experiment in a low-shear environment resulted in a

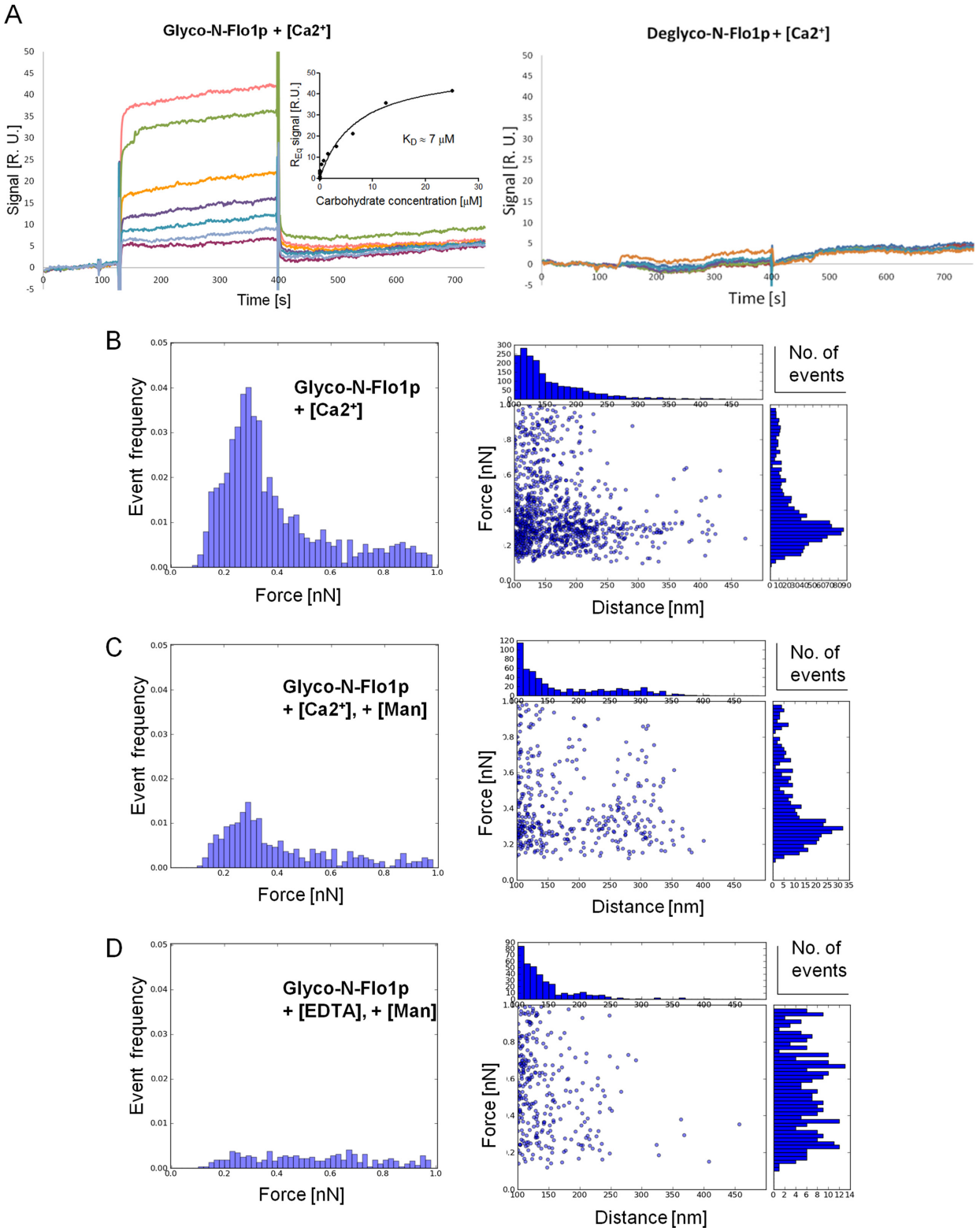

FIG 2 Analysis of N-Flo1p–N-Flo1p homophilic interactions. (A) N-Flo1p self-binding studied by SPR. N-Flo1p was immobilized on a CM5 chip, and 2-fold serial dilutions of an NFlo1p solution were injected (concentration range, 25 to 0.39 μM). (Left subpanel) Glycosylated N-Flo1p interaction in the presence of Ca^{2+}. The apparent K_D value of this interaction is calculated by using the response at equilibrium (R_{Eq}) values (concentration range, 25 μM to 1.5 nM) and a one-site binding model. (Right subpanel) Deglycosylated N-Flo1p interaction in the presence of Ca^{2+}. R.U., relative units. (B to D) AFM-force spectroscopy analysis data (see also Fig. S2 in the supplemental material). Force event histograms (left subpanels) and force-distance scatter plots (right subpanels), which correlate the unbinding distance to the unbinding force, illustrate glycosylated N-Flo1p self-binding (N-Flo1p on the tip versus N-Flo1p on the mica surface) obtained in liquid. (B) Tris solution with 10 mM $CaCl_2$. (C) Tris solution with 10 mM $CaCl_2$ and 100 mM mannose. (D) Tris solution with 20 mM EDTA and 100 mM mannose.

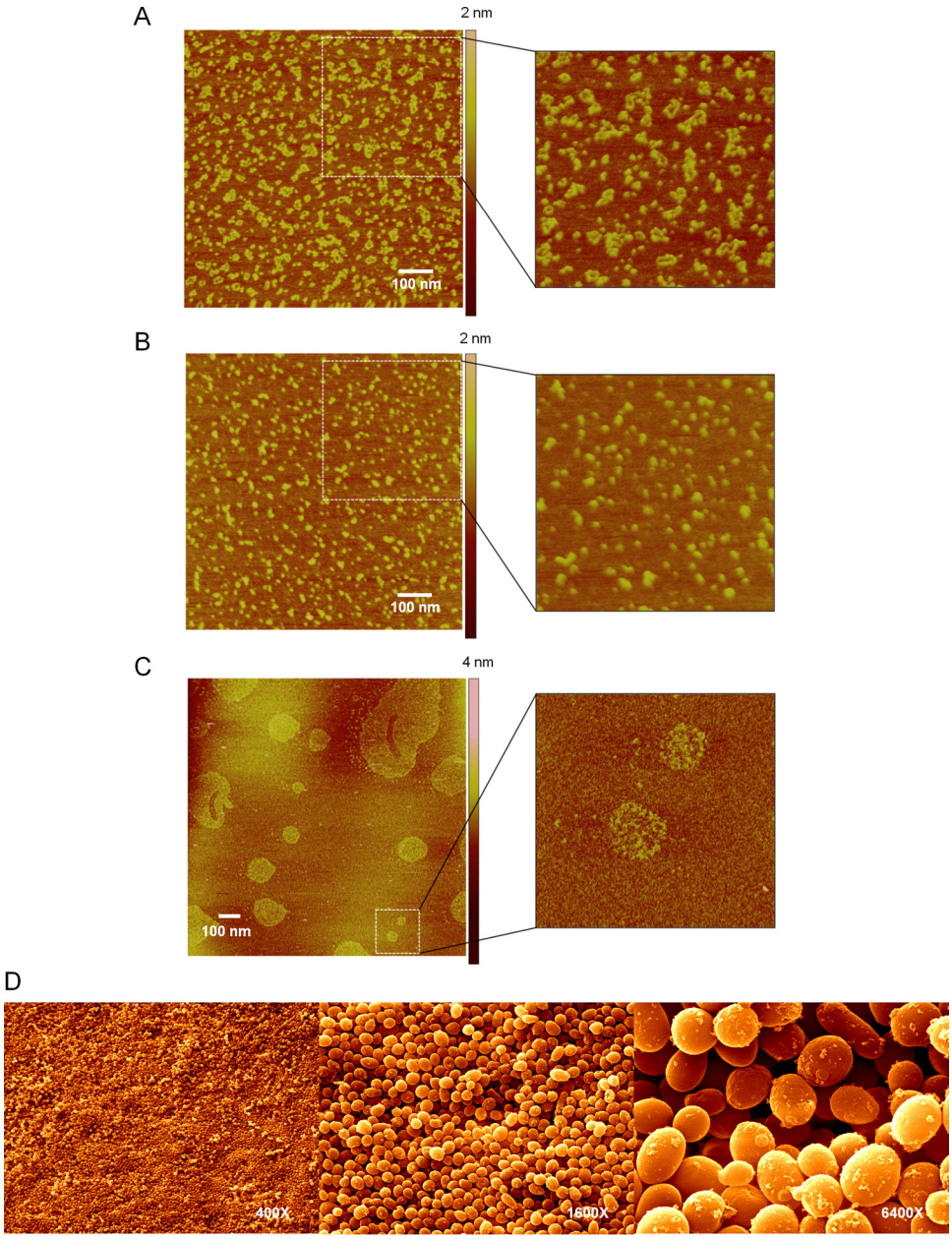

FIG 3 Imaging of N-Flo1p glycans and floc ultrastructure. (A) Single-molecule imaging of glycans in the presence of Ca^{2+} shows an elongated or closed-ring conformation; the right image is zoomed in (400 by 400 nm). (B) Imaging of glycans in the presence of EDTA. The glycans adopt a globular conformation; the right image is zoomed in (400 by 400 nm). (C) Aggregates of glycans are observable when the Ca^{2+}/glycan ratio is increased. The scan size of the right image is 2.0 μm. (D) Ultrastructure of a floc (BY4742 [*FLO1*]) by SEM imaging.

much higher number of differentially expressed genes for both flocculent strains than for the nonflocculent WT strain (Fig. 4; see also Fig. S4 and Table S2 in the supplemental material). This indicates that more cells were in the flocculent state and that nutrient limitation conditions were obtained earlier compared to growth at 1 *g*. This is consistent with a reduced total number of cells and a higher glucose concentration in the culture chamber at the end of the experiment under μg conditions than under 1-*g* conditions (Fig. 5A and B). The functional enrichment based on gene ontology (GO) annotation is presented in Fig. 4B, where it is shown that the processes related to flocculation were induced in both the *FLO1* overexpression strain and the BY4742::*FLO8* strain compared to the WT reference. This effect was seen under both growth conditions.

The genome-wide expression data were integrated on the high-confidence protein-protein interaction (PPI) network to search for differentially expressed high-score subnetworks leading to groups of important proteins that potentially cross talk with Flo1p and Flo8p. The high-score subnetwork seen under each growth condition is presented with its functional enrichments (see Fig. S4 in the supplemental material). Based on the statistical cutoff at an adjusted *P* value of 0.001, it is clearly seen that activation of *FLO8*

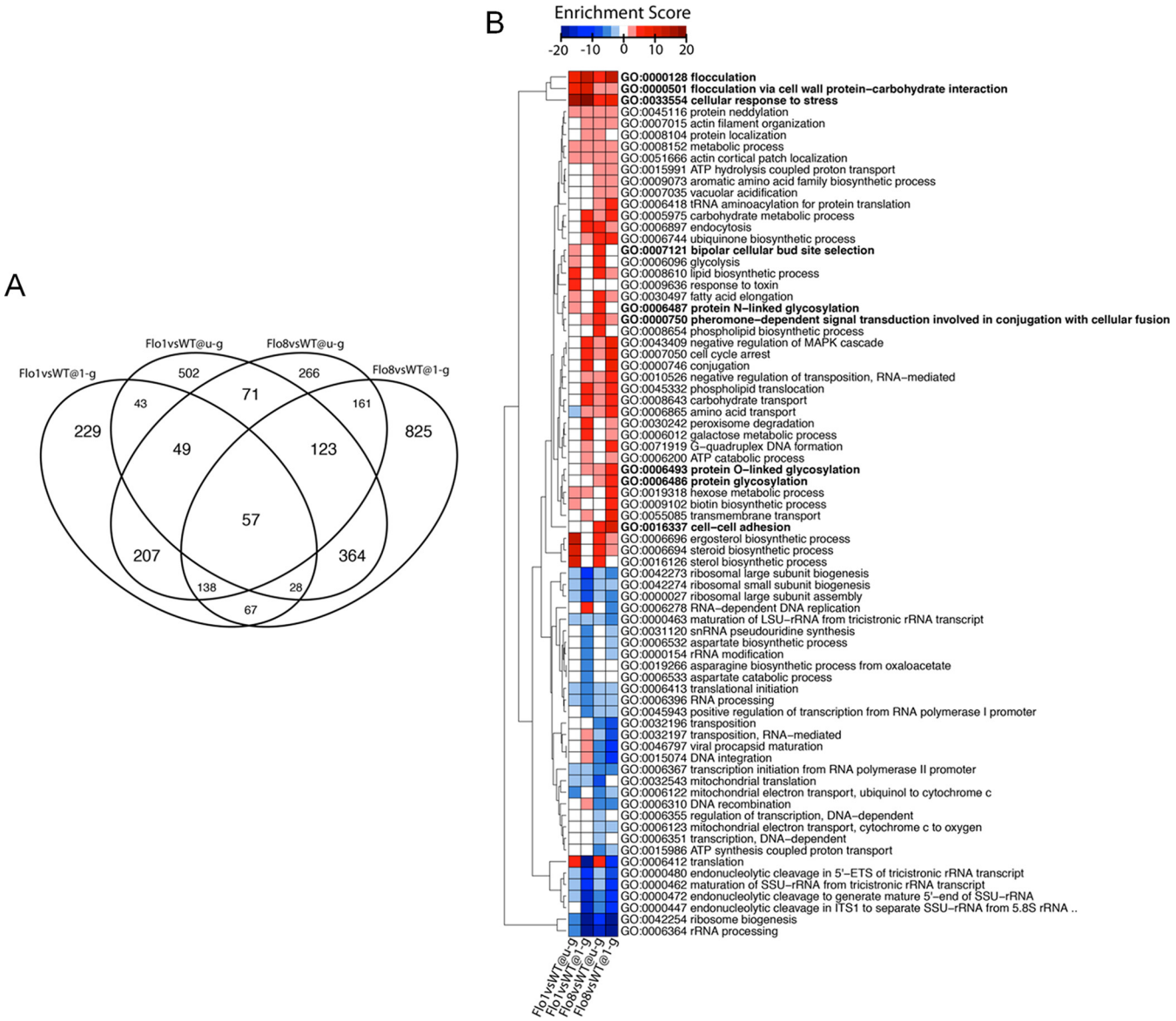

FIG 4 Transcriptome analysis and determination of the mating efficiency. (A) Differentially expressed genes (*Q* value of <0.05) in BY4741::*FLO8* and *FLO1* that were overexpressed compared to the levels seen with the BY WT strain under 1-*g* and μg conditions. (B) Heat map of functional enrichment analysis. The enrichment score (−log10 [enrichment *P* value]) data are shown in red for overrepresented gene ontology terms and in blue for the ones underrepresented in BY4741:: *FLO8* and *FLO1* that were overexpressed compared to the levels seen with the BY WT strain under 1-*g* and μg conditions. All gene ontology terms that had *P* values of <0.001 are shown (see also Fig. S4 in the supplemental material). LSU, large subunit; SSU, small subunit; ETS, external transcribed spacer.

has a bigger influence on the trajectory size of the identified high-score subnetworks than *FLO1* overexpression. Moreover, cultivation under a low-shear (μg) condition also increased the trajectory size of the identified high-score subnetworks, which makes this condition suitable for recognition of more subnetworks. Interestingly, the identified subnetworks are commonly enriched in processes related to flocculation and mating, suggesting a positive correlation between these two processes. Additionally, genes involved in mating-type switching, conjugation with cellular fusion, sporulation, response to decreased oxygen levels, and arrested growth are also enriched (see Table S2).

The link between flocculation and mating was experimentally confirmed by determining the mating efficiency (under 1-*g* conditions), which was performed under unstirred (mating assay on a filter and in nonshaken liquid) and stirred (shaken liquid) conditions. In all cases, it was shown that mating is more efficient ($P < 0.05$) when *FLO* genes are expressed, indicating that flocculation enhances mating efficiency (Fig. 5C).

DISCUSSION

The N-Flo1p and N-Lg-Flo1p mechanisms of interaction with mannosides are similar, but the ligand size is important in the choice of the binding partner. N-Flo1p shows a capacity for mannoside binding that is more efficient than that seen with N-Flo5p, although their apo form structures are almost identical in sequence and topology. Both contain a partially disordered L3 loop,

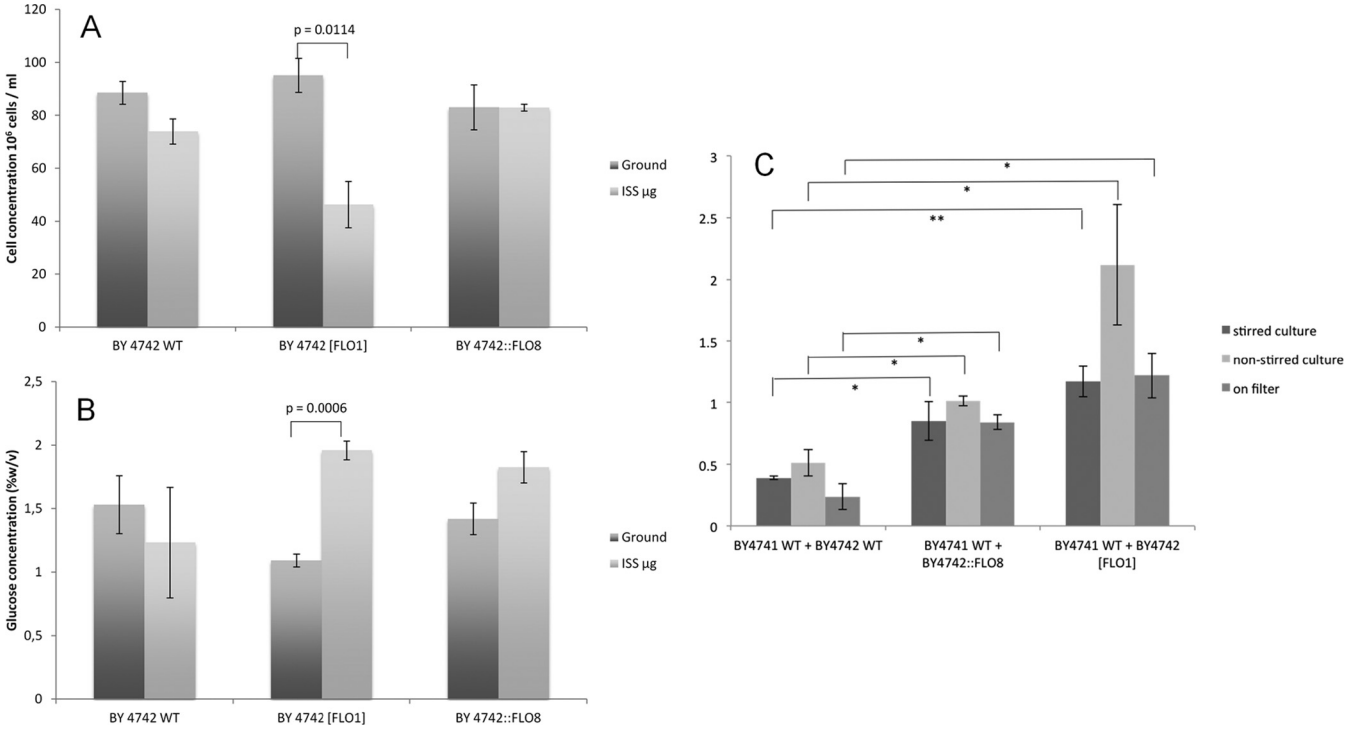

FIG 5 Cell growth and glucose consumption of *S. cerevisiae* strains grown under 1-*g* and μg conditions. (A) Cell concentrations determined at the end of the growth experiment in microgravity (μg) and at 1 *g* (ground). (B) Glucose concentrations (percent [wt/vol]) at the end of the growth experiment in μg and at 1 *g*. (C) Mating efficiency determined in stirred and nonstirred liquid and on a filter. The mating efficiency, determined by dividing the number of cells on SC-MK medium by the number on SC-M medium, is significantly higher with cells expressing *FLO* genes (*, $P < 0.05$; **, $P < 0.01$).

which is also present in the Epa1 adhesin from *Candida glabrata* as directly participating in the interaction with galactosides (25, 26). This loop plays a significant role in carbohydrate recognition and contributes to an affinity for mannose that is 3-fold higher than in the case of N-Flo5p. This is due to the fact that the side chain of K194 in N-Flo1p is close enough to the binding site to directly interact with the carbohydrate, in contrast to N-Flo5p. Its proximity to the axial 2′-OH on the mannopyranose ring suggests the contribution of K194 in determining the Flo1p carbohydrate specificity, together with the Q98 residue in the Flo1 subdomain. The conformation adopted by the L3 loop in the N-Flo1p–mannose complex is different from the one in bound N-Flo5p, which is due to the loop sequence variations between the two proteins; i.e., D202 in N-Flo5p is replaced by a proline in N-Flo1p. This would block L3 in a single preferred conformation and create favorable conditions for direct interactions of the loop side chains with the hexose without affecting the specificity. For N-Flo5p, a D202T mutation could also influence both ligand affinity and promiscuity by constraining L3 in a specific conformation (20). The shift in the L3 loop position, observed upon mannoside binding in N-Flo1p (not in N-Flo5p), is likely responsible for the increased affinity of N-Flo1p for mannose-containing carbohydrates. However, the variations in the binding equilibrium parameters between the two flocculins are not dramatic and the K_D values are still in the (sub)millimolar range. The approach of L3 to the CBL1 possibly requires an entropic cost for binding, which is compensated only by the specific interaction with mannose and its axial 2′-OH. In Epa1p, W198 (which corresponds to K194 in Flo1p) on L3 also plays a role in the recognition of galactose and galactose-terminating glycans (25, 26), and it establishes stronger stacking interactions with the ligand.

The same main structural features of N-Flo1p are found in N-Lg-Flo1p from *S. pastorianus*. However, an even more enclosed binding pocket accounts for a much higher affinity for mannose. This seems to come at a cost for the interaction with longer carbohydrates. There is a distinct variation in the way the disaccharide fits into the N-Lg-Flo1p active pocket compared to Flo5p-mannose (PDB code 2XJS) since the coordination of the Ca^{2+} ion takes place via the hydroxyl groups of the reducing moiety. Formation of the Ca^{2+}-mannobiose complex via the nonreducing end seems to be excluded, likely due to the steric hindrance of the long K199 side chain. The latter, together with W90 of L2, contributes to the shielding of the binding pocket from the solvent and the creating of a narrower hydrophobic environment. At the same time, the charged amino group on the same chain would readily establish an electrostatic interaction with the phosphate group of a mannose-1-phosphate residue, which is a micromolar-affinity ligand of N-Lg-Flo1p (21).

For N-Lg-Flo1p, the geometry of interaction with high-mannose glycans is different from that seen with N-Flo5p; i.e., it occurs through one of the α-1,6-linked mannoses, an interpretation that is justified by steric reasons. More remarkably, N-Lg-Flo1p does not appear to be "specialized" in the recognition of oligosaccharide molecules, despite its reduced solvent accessibility and the possibility for mannobioses to dock into the binding pocket. Longer mannose-containing molecules are more sterically demanding than mannose, and this is not counterbalanced by

strong interactions between the supplementary residues and the protein, which was confirmed by ligand affinity data (21).

The spectroscopic data not only clearly confirmed the influence of the L3 loop position and the conformation of all Flo structures on their interaction with carbohydrate ligands but also revealed the ability of N-Flo1p to recognize mannose oligosaccharides with different glycosidic linkages. The influence of monosaccharides on flocculation was previously assessed on the cellular level (5, 12, 28). Recently, molecular quantitative data were determined for N-Flo1p (22), for N-Flo5p (20), and for N-Lg-Flo1p (21).

The role of the N-Flo1p glycans in the self-binding of *S. cerevisiae* cells. The N-terminal domain of Flo1p is expressed as two populations with different molecular masses (22). In this study, we demonstrated that N-Flo1p contains three sites for O-glycosylation and three sites for N-glycosylation. The O-glycosylation sites are decorated with two mannoses, and the N-glycosylation sites contain both the core and the hyperglycosylated type N-glycans. However, the distributions of the two types of N-glycans differ in the two populations. The 36-kDa N-Flo1p population is decorated with two core type N-glycans and one hyperglycosylated N-glycan, while the 100-kDa population possesses two hyperglycosylated type N-glycans and one core type N-glycan.

SPR results revealed that N-Flo1p interacts homophylically with the glycans of N-Flo1p in the presence of Ca^{2+}. Self-interaction of N-Flo1p molecules was confirmed using AFM imaging (data not shown). The Flo proteins, which stick out of the cell wall, are the dominating cell wall proteins on flocculating yeast cells (16). Therefore, an interaction with glycans from other cell wall proteins is less likely to occur, and homophilic Flo protein interactions are almost exclusively responsible for the flocculation phenotype. The SPR data indicate that this interaction is characterized by micromolar affinity (Fig. 2A), and binding experiments confirm that the affinity of N-Flo1p for mannose is in the millimolar range (Fig. 1F). This low affinity guarantees that the occasional binding of Flo1 proteins to other Flo1 proteins on the same yeast cell is abolished quickly and allows Flo1p to then interact with neighboring cells. It was also hypothesized that binding with other Flo1 proteins on the same yeast cell is prevented due to the presence of two binding sites, since one binding site is supposed to form *cis* interactions, thereby immobilizing the N-terminal domain at the yeast surface, while the second binding site is responsible for the *trans* interactions (20).

Interestingly, Flo11p has also been demonstrated to possess homophilic adhesion ability (12, 13). Flo11p can compensate for Fig2p (2) when overexpressed, and Fig2p can interact homophylically with Fig2p during mating (29). These results indicate that cell-cell adhesive interactions during flocculation and agglutination are mostly established by homophilic interactions, which ensure species-specific formation of aggregates, as demonstrated in an experiment where the floc structure was preferentially composed of *FLO1*-expressing cells when *FLO1*$^+$ and *flo1* cells were mixed before aggregation (24). Cell-cell adhesion under conditions of shear force further sorts out the more weakly binding cells, which was demonstrated for interacting *Dictyostelium* cells via the csA adhesin (30).

The role of direct carbohydrate-carbohydrate interactions has not yet been explored in yeast flocculation. It was shown for sponge proteoglycans that carbohydrate-carbohydrate interactions can be important for cell adhesion phenomena since glycans occur on the outermost cell periphery and therefore are likely involved in the first intercellular contacts (31–34). Hence, the role of the glycans present on N-Flo1p in the flocculation event was further studied by analyzing the purified Flo1p glycans. Using AFM imaging, it is shown that glycans aggregate in the presence of Ca^{2+} (Fig. 3A to C). The initial steps in cell recognition and adhesion events by carbohydrate-carbohydrate interactions can be further reinforced by other intercellular interactions, e.g., lectin-carbohydrate interactions. The presence of these two types of interaction points to a two-stage cell-cell adhesion process. The long, flexible glycans have a high probability of interaction when cells are moving toward each other. These interactions stabilize the cell-cell interactions, allowing the nonreducing glycan ends to penetrate the binding pocket. Divalent Ca^{2+} cations play a crucial role in both types of interaction. These results show that the cell-cell adhesion mechanism for flocculating yeast cells is based on glycan-lectin binding as well as on glycan-glycan interactions (Fig. 6) and actually unify the generally accepted lectin hypothesis (35) with the historically first-proposed molecular cell flocculation mechanism, i.e., the "Ca^{2+}-bridge" hypothesis (36, 37). This hypothesis states that flocculation is based on ionic interactions stabilized by hydrogen bonds and on the involvement of Ca^{2+} ions that form bridges between flocculating cells by linking the carboxyl groups present on the cell surface. Our results show that Ca^{2+} can bridge cells through glycan-glycan interactions.

The role of Flo8p in flocculation. Flo8p was originally identified as a transcriptional activator of *FLO1*, and in addition, it was found that transcription of the *FLO11* (*MUC1*) and *STA1* (encoding extracellular glucoamylase) genes is also positively regulated by *FLO8* (38). Mutation in *FLO8* and mutation in the *MSS11* transcription factor show very similar phenotypes, and those genes coimmunoprecipitated and bound cooperatively to UAS1-2 of the *STA1* promoter (39, 40). The Flo8p transcriptional activation domain contains an N-terminal LisH motif that appears to be required for its physical interaction with the Mss11p transcription factor for cooperative transcriptional regulation of the shared targets (39–41). Flo8p and Mss11p can directly form either a heterodimer or a homodimer capable of binding to DNA, and the Flo8-Mss11 heterodimer interacts functionally and physically with the Swi/Snf complex, which is critical for activation of *STA1*, *FLO11*, and *FLO1* expression.

In the *FLO1*-overexpressing strain as well as in the Flo8p active strain, *FLO1* is upregulated. The most striking difference between the two strains is the expression of *FLO11* and the associated genes involved in its regulatory pathways in the Flo8p active strain. Numerous studies have revealed detailed insights into the complex topology of regulatory pathways at the promoter of *FLO11* and its responsiveness to many external and internal signals (42). The *FLO11* promoter is under the control of several conserved signaling cascades, including the cyclic AMP-protein kinase A (cAMP-PKA) pathway (43–49), the Fus3/Kss1-mitogen-activated protein kinase (MAPK) cascade (46, 50), the Snf1 pathway (51), the general amino acid control system (52), and the target of rapamycin (TOR) network (53). Although dynamic information is necessary to fully unravel the regulatory mechanisms involved, the low-shear transcriptomics data in particular sheds detailed light on *FLO11* regulation at the beginning of the stationary-growth phase (see C1 in Fig. S4 in the supplemental material). This microgravity experiment provides a unique extensive data set of differentially

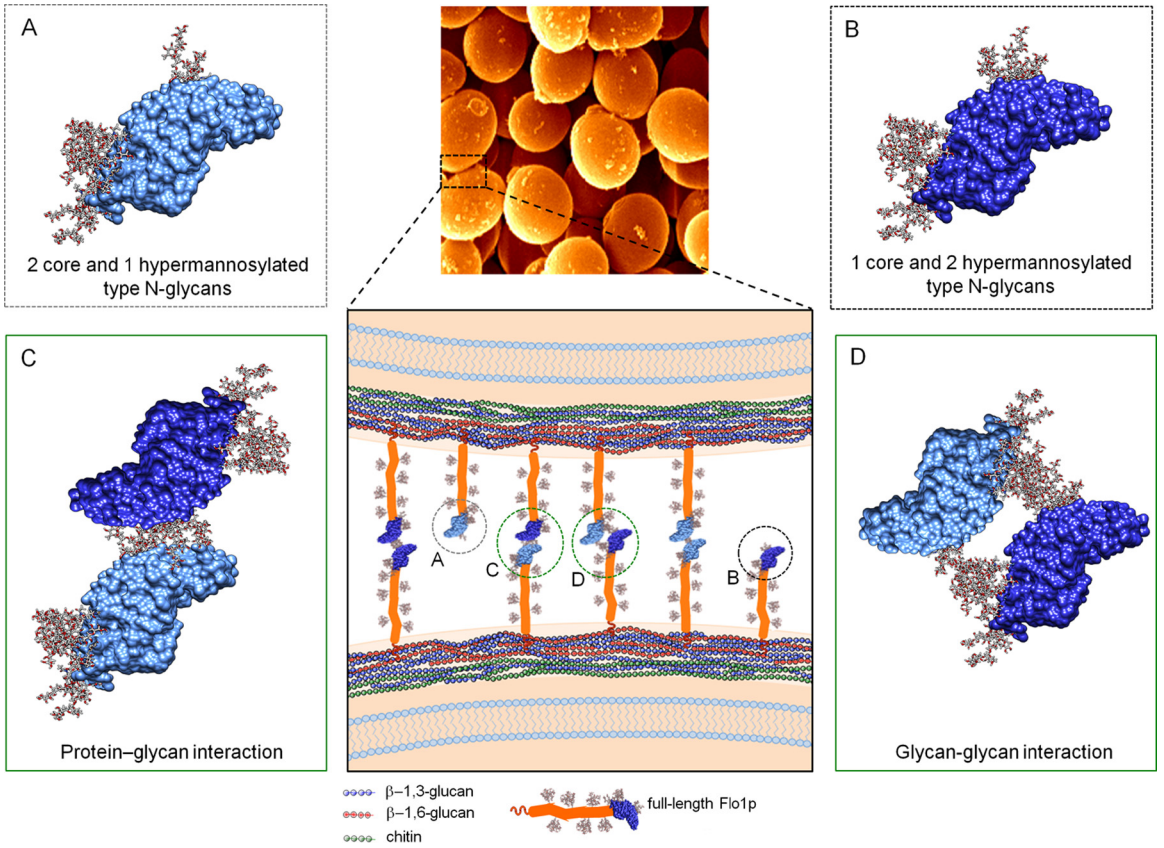

FIG 6 Molecular flocculation model based on Flo1p homophilic self-interaction. The two populations of N-Flo1p, which carry different types of N-glycans (see also Fig. S3 and S6 in the supplemental material), are illustrated. Two *S. cerevisiae* cells bind together via Flo1p self-interaction. This binding is accomplished via lectin-glycan and glycan-glycan interactions.

expressed genes that allows confirming many results of previous research and indicates new links in the regulation of *FLO11* expression and flocculation.

The low-shear μg results indicate glucose starvation and activation of the cAMP-PKA pathway by the downregulation of *FLO8* via the Tpk2p branch of the pathway, as well as by the upregulation of the transcription factors *PHD1* via the Tpk1p branch and *ASH1* of the pathway (see C1 and C2 in Fig. S4 in the supplemental material). The dual-specificity Yak1p protein kinase is at the center of a regulatory cascade for adhesive growth and stress resistance, which is under dual control of the Whi3p RNA-binding protein and the Tpk1 PKA subunit (49, 54). In our results (see C2 in Fig. S4), the downregulated *WHI3* is directly linked to the upregulated *FLO11* and Cdc28-Cln3p cyclin-dependent protein kinase, which plays a role in the control of the cell size at the G_1/S transition (55, 56). Whi3p is also linked to the cell cycle by controlling the production of the G_1 cyclins Cln1p and Cln2p and also targets, besides Tpk1, the Tec1p transcription factor (57), which is well known to activate *FLO11* expression (46, 58–60). It is also able to negatively control stress-regulated genes via a currently unknown repressor and might be able to control the stability of ploidy by affecting the expression of many genes involved in sister chromatid cohesion (57). Additionally, the differentially upregulated *SNF1* and *SNF4* genes in the network (see C2 and C3 in Fig. S4) also indicate glucose starvation (carbon stress) conditions and activation of the Snf1 protein kinase pathway (61–64). The detected upregulation of *FLO11* depends also on this Snf1 pathway (51, 65–69). In the Flo8 active subnetwork (see C3 in Fig. S4), *SNF1* is directly linked to the hexose transporters *HXT13* (upregulated) and *HXT3* and *HXT5* (downregulated). The Snf1p complex regulates several transcription factors that affect the expression of genes required for low-glucose-concentration consumption and alternative carbon sources (70–72), and its expression level is also affected by the concentration of available oxygen (73), which is depleted in a floc. Additionally, several genes linked to *SNF1* and involved in the regulation of glucose-repressible genes, such as *MTH1* (74), *CAT8* and *ADR1* (75–78), *REG2* (79–81), and *GAC1* (82, 83), are downregulated, which also is an indication of carbon stress. Glucose repression inhibits Adr1p activity by multiple mechanisms (84), including *ADR1* expression (85), DNA binding (86, 87), transcription activation (77, 88–90), and binding to 14-3-3 (Bmh) protein (91). Snf1p also controls *FLO11* expression by inactivating the transcriptional repressors Nrg1p and Nrg2p (92, 93). These repressors are under the control of the Dfg16-Rim101 pathway, which also indicates pH control of *FLO11* (94, 95). The RIM pathway was activated by the upregulation of *RIM101*, *RIM20*, and *VPS4* and by the downregulation of *DFG16* and *VPS20* in the Flo8p active low-shear data. In the *FLO1* overexpression low-shear μg data (see panel D in Fig. S4), *RIM101* was upregulated, but here *FLO11* was not expressed. Also, the upregulated *ASH1* in this data set did not activate *FLO11* expression. There is also no *FLO11* expression in the *FLO1* overexpression 1-*g*

data set, where *TEC1* and *FUS3* (MAPK pathway) are upregulated. These results indicate that these activated pathways in the *FLO1* overexpression strain are involved in activities other than *FLO11* expression, such as in mating (see the next section).

FLO11 expression is also activated by amino acid starvation and low glucose concentration (52, 96), which depends on the sensor kinase Gcn2p and the transcription factor Gcn4p, which are central elements of the general amino acid control (GAAC) system (97). However, Gcn4p seems to regulate *FLO11* indirectly in response to amino acid starvation (42, 52, 98). In the Flo8 active μg network, the GAAC pathway is activated and linked to the upregulated *FLO11* gene (see C4 in Fig. S4). The downregulated *GCN4* and *GCN2* genes are connected to the upregulated (*ARO4* and *SER1*) and downregulated (*LYS14*) genes involved in amino acid biosynthesis, as well as to *SUI1* and *TIF11*, which are involved in the translation control of *GCN4* (97). *GCN2* is directly linked to upregulated *ASC1*, which has been shown to be required for *FLO11*-dependent adhesive growth upon amino acid starvation in haploid cells (98). Asc1p impacts transcription factors in the MAP kinase pathways of invasive and filamentous growth and cell wall integrity (99, 100). Evidence of translational regulation of these pathway-targeted transcription factors (Flo8p, Ste12p, Tec1p, Rap1p, and Phd1p) suggests that ribosomal Asc1p controls the biosynthesis of the final transcription regulators.

In the Flo8 active μg network, *FLO8*, as well as *FLO11*, is directly linked to the downregulated protein kinase *HSL1* (101) and *CDC28* (see C1 and C4 in Fig. S4 in the supplemental material). Hsl1p has a role in delaying the cell cycle in G_2 phase as a response to sudden (stressful) environmental changes by recruiting the Wee1-family kinase Swe1p via the bridging action of Hsl7p to the septin collar (102–104). Following stress, feedback between Swe1p and Cdc28p controls Swe1p abundance, which promotes a delay in nuclear division that is thought to maintain coordination between budding and the nuclear cycle (105, 106). Previously, it was shown that inactivation of Hsl1p is sufficient to promote filamentous growth caused by inactivation of Flo8p or Tec1p but is insufficient to promote filamentous growth in the absence of both factors (107). Our results also indicate the involvement of this morphogenesis checkpoint in yeast flocculation.

The general stress activator protein Yap1p was a key mediator of *FLO11* expression that was induced by adding the plant hormone indole acetic acid (IAA) (108). In the Flo8p active network (see C5 in Fig. S4 in the supplemental material), *YAP1* is differentially expressed (downregulated) and is linked to *GCN2*, *FLO8*, *FLO11*, and *FLO1* via *EPL1*. Epl1p is a subunit for NuA4 (nucleosome acetyltransferase of H4) (109) and is thus involved in epigenetic regulation. Epl1p is linked—via *HTZ1* (gene of histone variant H2AZ)—to *RPN4*, which is a transcription factor that stimulates the expression of proteasome subunit genes as well as of genes involved in ubiquitylation, DNA repair, and other stress responses (110). *RPN4* expression is also subject to control by Yap1p (111). Several other proteins involved in epigenetic regulation processes, such as histone acetylation (Taf12p and Ahc1p [SAGA complex], Taf12p [NuA3], Epl1p, Yng2p, and Act1p [NuA4], Iki3p [elongator complex of polymerase II, and the TFIID subunit Taf1p]), histone deacetylation (Sin3p [RPD3L] and Sir2p [SIR]), and histone ubiquitination (Bre1p), are differentially expressed in this network. Epigenetic regulation of *FLO11* expression via the Rpd3L complex has been described previously (95, 112). Another mechanism that depends on the regulator Sfl1p and the histone deacetylase complex (HDAC) has also been reported (113).

The role of flocculation in mating and survival. Differences in gene expression between flocculating strains (BY4742::*FLO8* and *FLO1* overexpression strains) and the nonflocculating BY4742 WT strain under 1-*g* and μg growth conditions were investigated by transcriptome analysis. This analysis showed that flocculation genes and genes involved in the mating process are coexpressed (Fig. 4; see also Fig. S4 in the supplemental material), which indicates that mating is induced in flocs. Various genes involved in "conjugation with cellular fusion" (see Table S2), including the genes involved in pheromone production [*MF*(*ALPHA*)*2*], a receptor protein (*STE3*) and associated G proteins (*GPA1*, *STE4*, and *STE18*), signal transduction via the MAPK pathway (*STE7*, *FAR1*, and *FUS3*), sexual adhesins (*AGA2* and *SAG1*), and cell (*PRM1* and *FIG1*) and nuclear (*PRM2*) fusion (114–118), are differentially expressed. Interestingly, the 1-*g* data set (see Fig. S4B) and the Flo8 active μg data set (see Fig. S4C) from the *FLO1* overexpression strain show clearly the link between mating and flocculation by the upregulation of many genes involved in these processes. Since Flo8p is not active in the *FLO1* overexpression strain, these results indicate that active Flo8p is not necessary to induce mating but that specific microenvironmental conditions that are present in the floc are needed.

These transcriptomics results were confirmed experimentally by mating assays (Fig. 5C). These assays showed that *MAT*α cells with active Flo8p or overexpressed Flo1p mated with WT *MAT***a** had a higher mating efficiency than the WT mating pair. The highest mating efficiency was obtained for the Flo1p-overexpressing strain, although there were no significant differences among the flocculating strains under all 3 conditions. This means that—due to cell immobilization in the floc structure—the mating efficiency became independent of the shear flow and that mating was as efficient under liquid conditions as on a solid substrate. This finding is of major importance with respect to the role of flocculation in the survival of yeast cells under starvation conditions as it enhances the mating efficiency. The results of the mating assays indicate that the role of Flo proteins and flocculation in mating is the construction of a uniquely organized multicellular ultrastructure (the floc) that ensures tight cell adhesion, which is necessary for zygote formation. This is consistent with the observed structure of an induced cell aggregation pellet, which was solely based on agglutinin interaction, where it was shown that sexual agglutination contributes not only to cell contact between *MAT***a** and *MAT*α *AG*α*1* cells, thereby stabilizing **a**-α cell pairs, but also to the construction of a uniquely organized ultrastructure (119). The interaction between the sex agglutinins, which are localized at the outermost cell wall surface (115) (comparable to the localization of the flocculins), was responsible for the formation of this "extended" ultrastructure, which provides the gametic cells with nutrients and is beneficial for subsequent growth of diploid cells. The ultrastructure of this extended type aggregate is comparable to the floc ultrastructure (Fig. 3D). In contrast to flocculation, a physical method (centrifugation) was needed to create this agglutination ultrastructure. Therefore, cell-cell interaction based on the stronger lectin-carbohydrate binding is the natural way of creating this mating-favorable ultrastructure.

Due to diffusive mass transport limitations in a floc (120), nitrogen and carbon sources as well as oxygen drop to limiting concentrations inside the floc. This was confirmed by the tran-

scriptome analysis: upregulation of genes involved with GO "gluconeogenesis" and "pentose-phosphate shunt" and genes involved in GO "response to starvation" and "autophagy" (see Table S2 in the supplemental material). Additionally, many genes involved in cell wall, lipid, sphingolipid, and sterol metabolism are upregulated. Anaerobic conditions are indicated by the upregulation of the Tir, Pau, and Dan mannoproteins, the upregulation of *AAC3* and *HEM13*, and downregulation of *ROX1*. This is consistent with previous transcriptome results obtained with *FLO1*-overexpressing cells (24). The reduced growth is confirmed by the downregulation of genes involved with RNA processing and ribosome synthesis. Severe limitation of both nitrogen and fermentable carbon sources and increased pH induce diploid cells to sporulate (121, 122). This is confirmed by the transcriptome analysis: upregulation of genes associated with GO "sporulation" (including the involvement of TOR signaling and SNF1 signaling) and Rim101 pathway activation (see Table S2). These results confirm a previous transcriptome analysis, where genes associated with GO "sporulation" and "spore wall assembly" were also differentially upregulated in *FLO1*-overexpressed flocs (24). Also, several of the enriched differentially expressed genes that are associated with yeast flocculation (see Table S2) are also enriched in yeast biofilms and colonies (11, 121, 123–125).

Flocculation is thus of crucial importance for the enhanced chance of survival of Flo-expressing yeast cells under sustained stress conditions. The benefits of flocculation with respect to cell survival are manifold: flocculation gives the cells a way to escape from harsh conditions in the growth medium, a floc protects the inner cells from environmental stress, and cells in the middle of the floc could lyse and act as a source of new nutrients for the other cells (24). The new findings concerning the increased mating efficiency in a floc suggest an additional role of flocculation in survival. Mating results in an offspring with genetic variation. Additionally, diploid cells can undergo meiosis and sporulation and can package the haploid nuclei into spores to increase the survival rate, since spores are highly resistant to a variety of environmental stresses (121, 122). Therefore, flocculating cells have a significantly higher chance for survival than nonflocculent cells.

MATERIALS AND METHODS

Expression and purification of the lectin domain of Flo1p and Lg-Flo1p. The glycosylated N-terminal domain of Flo1p was purified by a combination of affinity chromatography and gel filtration after expression in *S. cerevisiae* (22). Expression and purification of the N-terminal domain of Flo1p and Lg-Flo1p from *Escherichia coli* have been described elsewhere (126) (see Text S1 in the supplemental material).

Protein crystallization and X-ray structure determination. Crystallization and X-ray data collection for N-Flo1p (in apo form and in complex with mannose) and N-Lg-Flo1p (in complex with α-1,2-mannobiose) have been described elsewhere (126). The structure of the flocculin N-terminal domains (PDB codes 4LHK [N-Lg-Flo1p–mannobiose], 4LHL [apo–N-Flo1p], and 4LHN [N-Flo1p–mannose]) were solved by molecular replacement (see Text S1 and Table S1 in the supplemental material).

Enzymatic deglycosylation and glycan preparation. The N-glycans were removed with endo-β-*N*-acetylglucosaminidase H and the O-glycans with α-mannosidase from *Canavalia ensiformis*. To obtain deglycosylated protein only, the glycans were separated by dialysis; to obtain the glycans only, the deglycosylated protein was precipitated with ice-cold ethanol (see Text S1).

ESI-MS and N-glycan profiling. Glycosylated N-Flo1p, N-deglycosylated N-Flo1p, and both N-deglycosylated and O-deglycosylated N-Flo1p were analyzed with electrospray ionization-mass spectrometry (ESI-MS). The proteins were eluted from the column by isocratic elution followed by a linear gradient. The data were analyzed with Masslynx software version 4.1. The N-glycans were analyzed using high-pH anion-exchange chromatography with pulsed amperometric detection (HPAEC-PAD) and a CarboPac PA-200 column (see Text S1 in the supplemental material).

SPR. The self-interaction of N-Flo1p was studied by surface plasmon resonance (SPR) using a Biacore 3000 instrument (GE Healthcare, Uppsala, Sweden) (see Text S1 in the supplemental material).

AFM and SEM. Topographic images of the released N-glycans of the 100-kDa N-Flo1p population were recorded with atomic force microscopy (AFM) using the tapping mode in air. Samples for force spectroscopy were prepared by using a protein coupling method based on amino group chemistry, and force spectroscopy experiments were conducted in buffer solution (see Text S1 in the supplemental material). Glycosylated N-Flo1p was immobilized on both freshly cleaved mica and AFM tips. Detailed procedures for AFM and scanning electron microscopy (SEM) are described in Text S1.

For SEM imaging, yeast flocs were fixed in 2% (vol/vol) glutaraldehyde in Na-cacodylate buffer (0.1 M, pH 7) during 15 min at room temperature. The samples were then dehydrated with increasing ethanol concentrations (70%, 80%, 90%, and 100% [vol/vol]) for 10 min each time and immersed in hexamethyldisilazane (Sigma) for 3 min at room temperature. Samples were mounted on glass coverslips that were attached on aluminum stubs with silver paint, sputter coated with a layer (~8 nm thick) of Au/Pd, and examined with a Philips XL 20 SEM (FEI Company).

Microarray and network analysis. The BY4742 WT, BY4742::*FLO8*, and BY4742 [*FLO1*] (5) strains were grown in a specially developed bioreactor (see Fig. S5 in the supplemental material) (Kayser Italia, Leghorn, Italy) in microgravity and on Earth (see Text S1). The cells were fixed with RNA*Later*, and RNA was extracted. Next, each sample was amplified, labeled, and hybridized onto an Affymetrix Yeast Genome 2.0 array for the gene expression profiling. The differential gene expression analysis was performed using the moderate *t* test method (127) for different comparisons. The gene ontology (GO) enrichment analysis of different statistical hypotheses was performed using the R package PIANO (128). The high-quality protein-protein interaction networks were retrieved from the String Database (129), and the transcriptome data were integrated with the network.

Determination of the mating efficiency. The mating efficiency was determined by a genetic complementation assay (117). The following mating combinations were selected: BY4741 WT *MAT***a** and BY4742 WT *MAT*α; BY4741 WT *MAT***a** and BY4742::*FLO8 MAT*α; and BY4741 WT *MAT***a** and BY4742 [*FLO1*] *MAT*α.

Microarray data accession number. The microarray data have been deposited in NCBI's Gene Expression Omnibus (130) and are accessible through GEO Series accession number GSE64468.

SUPPLEMENTAL MATERIAL

Supplemental material for this article may be found at http://mbio.asm.org/lookup/suppl/doi:10.1128/mBio.00427-15/-/DCSupplemental.

Text S1, DOCX file, 0.1 MB.
Figure S1, DOCX file, 1.7 MB.
Figure S2, DOCX file, 0.1 MB.
Figure S3, DOCX file, 0.1 MB.
Figure S4, PDF file, 2.8 MB.
Figure S5, PDF file, 1.9 MB.
Figure S6, PDF file, 0.4 MB.
Table S1, DOCX file, 0.04 MB.
Table S2, DOCX file, 0.04 MB.

ACKNOWLEDGMENTS

The Belgian Federal Science Policy Office (Belspo), the Hercules Foundation (AUGE019), the European Space Agency (ESA) PRODEX program, and the Research Council of the Vrije Universiteit Brussel supported this work. We are grateful to ESA/ESTEC (Noordwijk, the Netherlands), the

Microgravity User Support Center (MUSC, Cologne, Germany), the Biotechnology Space Support Centre (BIOTESC, Lucerne, Switzerland), Kayser Italia (Leghorn, Italy), and EADS (Germany) as well as to the Belgian astronaut Frank De Winne for support of the flight experiment in the International Space Station. We thank González, Van Driessche, for support in mass spectrometric analysis. K.V.Y.G. and F.S.I. acknowledge the IWT (Belgium) for their Ph.D. grants.

REFERENCES

1. **Teunissen AW, Steensma HY.** 1995. Review: the dominant flocculation genes of *Saccharomyces cerevisiae* constitute a new subtelomeric gene family. Yeast **11:**1001–1013. http://dx.doi.org/10.1002/yea.320111102.
2. **Guo B, Styles CA, Feng Q, Fink GR.** 2000. A *Saccharomyces* gene family involved in invasive growth, cell-cell adhesion, and mating. Proc Natl Acad Sci U S A **97:**12158–12163. http://dx.doi.org/10.1073/pnas.220420397.
3. **Hoyer LL.** 2001. The *ALS* gene family of *Candida albicans*. Trends Microbiol **9:**176–180. http://dx.doi.org/10.1016/S0966-842X(01)01984-9.
4. **Lo WS, Dranginis AM.** 1998. The cell surface flocculin Flo11 is required for pseudohyphae formation and invasion by *Saccharomyces cerevisiae*. Mol Biol Cell **9:**161–171. http://dx.doi.org/10.1091/mbc.9.1.161.
5. **Van Mulders SE, Christianen E, Saerens SM, Daenen L, Verbelen PJ, Willaert R, Verstrepen KJ, Delvaux FR.** 2009. Phenotypic diversity of Flo protein family-mediated adhesion in *Saccharomyces cerevisiae*. FEMS Yeast Res **9:**178–190. http://dx.doi.org/10.1111/j.1567-1364.2008.00462.x.
6. **Stratford M, Assinder S.** 1991. Yeast flocculation: Flo1 and NewFlo phenotypes and receptor structure. Yeast **7:**559–574. http://dx.doi.org/10.1002/yea.320070604.
7. **Kobayashi O, Hayashi N, Kuroki R, Sone H.** 1998. Region of Flo1 proteins responsible for sugar recognition. J Bacteriol **180:**6503–6510.
8. **Govender P, Domingo JL, Bester MC, Pretorius IS, Bauer FF.** 2008. Controlled expression of the dominant flocculation genes *FLO1*, *FLO5*, and *FLO11* in *Saccharomyces cerevisiae*. Appl Environ Microbiol **74:**6041–6052. http://dx.doi.org/10.1128/AEM.00394-08.
9. **Lambrechts MG, Bauer FF, Marmur J, Pretorius IS.** 1996. Muc1, a mucin-like protein that is regulated by Mss10, is critical for pseudohyphal differentiation in yeast. Proc Natl Acad Sci U S A **93:**8419–8424. http://dx.doi.org/10.1073/pnas.93.16.8419.
10. **Purevdorj-Gage B, Orr ME, Stoodley P, Sheehan KB, Hyman LE.** 2007. The role of *FLO11* in *Saccharomyces cerevisiae* biofilm development in a laboratory based flow-cell system. FEMS Yeast Res **7:**372–379. http://dx.doi.org/10.1111/j.1567-1364.2006.00189.x.
11. **Bojsen RK, Andersen KS, Regenberg B.** 2012. *Saccharomyces cerevisiae*—a model to uncover molecular mechanisms for yeast biofilm biology. FEMS Immunol Med Microbiol **65:**169–182. http://dx.doi.org/10.1111/j.1574-695X.2012.00943.x.
12. **Douglas LM, Li L, Yang Y, Dranginis AM.** 2007. Expression and characterization of the flocculin Flo11/Muc1, a *Saccharomyces cerevisiae* mannoprotein with homotypic properties of adhesion. Eukaryot Cell **6:**2214–2221. http://dx.doi.org/10.1128/EC.00284-06.
13. **Goossens KV, Willaert RG.** 2012. The N-terminal domain of the Flo11 protein from *Saccharomyces cerevisiae* is an adhesin without mannose-binding activity. FEMS Yeast Res **12:**78–87. http://dx.doi.org/10.1111/j.1567-1364.2011.00766.x.
14. **Verstrepen KJ, Klis FM.** 2006. Flocculation, adhesion and biofilm formation in yeasts. Mol Microbiol **60:**5–15. http://dx.doi.org/10.1111/j.1365-2958.2006.05072.x.
15. **Dranginis AM, Rauceo JM, Coronado JE, Lipke PN.** 2007. A biochemical guide to yeast adhesins: glycoproteins for social and antisocial occasions. Microbiol Mol Biol Rev **71:**282–294. http://dx.doi.org/10.1128/MMBR.00037-06.
16. **Bony M, Thines-Sempoux D, Barre P, Blondin B.** 1997. Localization and cell surface anchoring of the *Saccharomyces cerevisiae* flocculation protein Flo1p. J Bacteriol **179:**4929–4936.
17. **Rigden DJ, Mello LV, Galperin MY.** 2004. The PA14 domain, a conserved all-beta domain in bacterial toxins, enzymes, adhesins and signaling molecules. Trends Biochem Sci **29:**335–339. http://dx.doi.org/10.1016/j.tibs.2004.05.002.
18. **Yoshida E, Hidaka M, Fushinobu S, Koyanagi T, Minami H, Tamaki H, Kitaoka M, Katayama T, Kumagai H.** 2010. Role of a PA14 domain in determining substrate specificity of a glycoside hydrolase family 3 β-glucosidase from *Kluyveromyces marxianus*. Biochem J **431:**39–49. http://dx.doi.org/10.1042/BJ20100351.
19. **Silipo A, Larsbrink J, Marchetti R, Lanzetta R, Brumer H, Molinaro A.** 2012. NMR spectroscopic analysis reveals extensive binding interactions of complex xyloglucan oligosaccharides with the *Cellvibrio japonicus* glycoside hydrolase family 31 α-xylosidase. Chemistry **18:**13395–13404. http://dx.doi.org/10.1002/chem.201200488.
20. **Veelders M, Brückner S, Ott D, Unverzagt C, Mösch HU, Essen LO.** 2010. Structural basis of flocculin-mediated social behavior in yeast. Proc Natl Acad Sci U S A **107:**22511–22516. http://dx.doi.org/10.1073/pnas.1013210108.
21. **Sim L, Groes M, Olesen K, Henriksen A.** 2013. Structural and biochemical characterization of the N-terminal domain of flocculin Lg-Flo1p from *Saccharomyces pastorianus* reveals a unique specificity for phosphorylated mannose. FEBS J **280:**1073–1083. http://dx.doi.org/10.1111/febs.12102.
22. **Goossens KV, Stassen C, Stals I, Donohue DS, Devreese B, De Greve H, Willaert RG.** 2011. The N-terminal domain of the Flo1 flocculation protein from *Saccharomyces cerevisiae* binds specifically to mannose carbohydrates. Eukaryot Cell **10:**110–117. http://dx.doi.org/10.1128/EC.00185-10.
23. **Straver MH, Smit G, Kijne JW.** 1994. Purification and partial characterization of a flocculin from brewer's yeast. Appl Environ Microbiol **60:**2754–2758.
24. **Smukalla S, Caldara M, Pochet N, Beauvais A, Guadagnini S, Yan C, Vinces MD, Jansen A, Prevost MC, Latgé JP, Fink GR, Foster KR, Verstrepen KJ.** 2008. *FLO1* is a variable green beard gene that drives biofilm-like cooperation in budding yeast. Cell **135:**726–737. http://dx.doi.org/10.1016/j.cell.2008.09.037.
25. **Ielasi FS, Decanniere K, Willaert RG.** 2012. The epithelial adhesin 1 (Epa1p) from the human-pathogenic yeast *Candida glabrata*: structural and functional study of the carbohydrate-binding domain. Acta Crystallogr D Biol Crystallogr **68:**210–217. http://dx.doi.org/10.1107/S0907444911054898.
26. **Maestre-Reyna M, Diderrich R, Veelders MS, Eulenburg G, Kalugin V, Brückner S, Keller P, Rupp S, Mösch HU, Essen LO.** 2012. Structural basis for promiscuity and specificity during *Candida glabrata* invasion of host epithelia. Proc Natl Acad Sci U S A **109:**16864–16869. http://dx.doi.org/10.1073/pnas.1207653109.
27. **Gupta R, Brunak S.** 2002. Prediction of glycosylation across the human proteome and the correlation to protein function. Pac Symp Biocomput **7:**310–322.
28. **Soares EV, Vroman A, Mortier J, Rijsbrack K, Mota M.** 2004. Carbohydrate carbon sources induce loss of flocculation of an ale-brewing yeast strain. J Appl Microbiol **96:**1117–1123. http://dx.doi.org/10.1111/j.1365-2672.2004.02240.x.
29. **Huang G, Dougherty SD, Erdman SE.** 2009. Conserved WCPL and CX4C domains mediate several mating adhesin interactions in *Saccharomyces cerevisiae*. Genetics **182:**173–189. http://dx.doi.org/10.1534/genetics.108.100073.
30. **Ponte E, Bracco E, Faix J, Bozzaro S.** 1998. Detection of subtle phenotypes: the case of the cell adhesion molecule csA in *Dictyostelium*. Proc Natl Acad Sci U S A **95:**9360–9365. http://dx.doi.org/10.1073/pnas.95.16.9360.
31. **Spillmann D, Burger MM.** 1996. Carbohydrate-carbohydrate interactions in adhesion. J Cell Biochem **61:**562–568. http://dx.doi.org/10.1002/(SICI)1097-4644(19960616)61:4<562::AID-JCB9>3.0.CO;2-M.
32. **Haseley SR, Vermeer HJ, Kamerling JP, Vliegenthart JFG.** 2001. Carbohydrate self-recognition mediates marine sponge cellular adhesion. Proc Natl Acad Sci U S A **98:**9419–9424. http://dx.doi.org/10.1073/pnas.151111298.
33. **Bucior I, Burger MM.** 2004. Carbohydrate-carbohydrate interactions in cell recognition. Curr Opin Struct Biol **14:**631–637. http://dx.doi.org/10.1016/j.sbi.2004.08.006.
34. **Fernàndez-Busquets X, Körnig A, Bucior I, Burger MM, Anselmetti D.** 2009. Self-recognition and Ca^{2+}-dependent carbohydrate-carbohydrate cell adhesion provide clues to the Cambrian explosion. Mol Biol Evol **26:**2551–2561. http://dx.doi.org/10.1093/molbev/msp170.
35. **Miki BL, Poon NH, James AP, Seligy VL.** 1982. Possible mechanism for flocculation interactions governed by gene *FLO1* in *Saccharomyces cerevisiae*. J Bacteriol **150:**878–889.
36. **Mill PJ.** 1964. The nature of the interactions between flocculent cells in

the flocculation of *Saccharomyces cerevisiae*. J Gen Microbiol **35:**61–68. http://dx.doi.org/10.1099/00221287-35-1-61.
37. **Jayatissa PM, Rose AH.** 1976. Role of wall phosphomannan in flocculation of *Saccharomyces cerevisiae*. J Gen Microbiol **96:**165–174. http://dx.doi.org/10.1099/00221287-96-1-165.
38. **Kobayashi O, Yoshimoto H, Sone H.** 1999. Analysis of the genes activated by the *FLO8* gene in *Saccharomyces cerevisiae*. Curr Genet **36:**256–261. http://dx.doi.org/10.1007/s002940050498.
39. **Kim TS, Ahn JY, Yoon JH, Kang HS.** 2003. *STA10* repression of *STA* gene expression is caused by a defective activator, *flo8*, in *Saccharomyces cerevisiae*. Curr Genet **44:**261–267. http://dx.doi.org/10.1007/s00294-003-0447-7.
40. **Kim TS, Kim HY, Yoon JH, Kang HS.** 2004. Recruitment of the Swi/Snf complex by Ste12-Tec1 promotes Flo8-Mss11-mediated activation of *STA1* expression. Mol Cell Biol **24:**9542–9556. http://dx.doi.org/10.1128/MCB.24.21.9542-9556.2004.
41. **Kim HY, Lee SB, Kang HS, Oh GT, Kim T.** 2014. Two distinct domains of Flo8 activator mediates its role in transcriptional activation and the physical interaction with Mss11. Biochem Biophys Res Commun **449:**202–207. http://dx.doi.org/10.1016/j.bbrc.2014.04.161.
42. **Brückner S, Mösch HU.** 2012. Choosing the right lifestyle: adhesion and development in *Saccharomyces cerevisiae*. FEMS Microbiol Rev **36:**25–58. http://dx.doi.org/10.1111/j.1574-6976.2011.00275.x.
43. **Robertson LS, Fink GR.** 1998. The three yeast A kinases have specific signaling functions in pseudohyphal growth. Proc Natl Acad Sci U S A **95:**13783–13787. http://dx.doi.org/10.1073/pnas.95.23.13783.
44. **Pan X, Heitman J.** 1999. Cyclic AMP-dependent protein kinase regulates pseudohyphal differentiation in *Saccharomyces cerevisiae*. Mol Cell Biol **19:**4874–4887.
45. **Pan X, Heitman J.** 2002. Protein kinase A operates a molecular switch that governs yeast pseudohyphal differentiation. Mol Cell Biol **22:**3981–3993. http://dx.doi.org/10.1128/MCB.22.12.3981-3993.2002.
46. **Rupp S, Summers E, Lo HJ, Madhani H, Fink G.** 1999. MAP kinase and cAMP filamentation signaling pathways converge on the unusually large promoter of the yeast *FLO11* gene. EMBO J **18:**1257–1269. http://dx.doi.org/10.1093/emboj/18.5.1257.
47. **Robertson LS, Causton HC, Young RA, Fink GR.** 2000. The yeast A kinases differentially regulate iron uptake and respiratory function. Proc Natl Acad Sci U S A **97:**5984–5988. http://dx.doi.org/10.1073/pnas.100113397.
48. **Conlan RS, Tzamarias D.** 2001. Sfl1 functions via the co-repressor Ssn6-Tup1 and the cAMP-dependent protein kinase Tpk2. J Mol Biol **309:**1007–1015. http://dx.doi.org/10.1006/jmbi.2001.4742.
49. **Malcher M, Schladebeck S, Mösch HU.** 2011. The Yak1 protein kinase lies at the center of a regulatory cascade affecting adhesive growth and stress resistance in *Saccharomyces cerevisiae*. Genetics **187:**717–730. http://dx.doi.org/10.1534/genetics.110.125708.
50. **Madhani HD, Galitski T, Lander ES, Fink GR.** 1999. Effectors of a developmental mitogen-activated protein kinase cascade revealed by expression signatures of signaling mutants. Proc Natl Acad Sci U S A **96:**12530–12535. http://dx.doi.org/10.1073/pnas.96.22.12530.
51. **Kuchin S, Vyas VK, Carlson M.** 2002. Snf1 protein kinase and the repressors Nrg1 and Nrg2 regulate *FLO11*, haploid invasive growth, and diploid pseudohyphal differentiation. Mol Cell Biol **22:**3994–4000. http://dx.doi.org/10.1128/MCB.22.12.3994-4000.2002.
52. **Braus GH, Grundmann O, Brückner S, Mösch HU.** 2003. Amino acid starvation and Gcn4p regulate adhesive growth and *FLO11* gene expression in *Saccharomyces cerevisiae*. Mol Biol Cell **14:**4272–4284. http://dx.doi.org/10.1091/mbc.E03-01-0042.
53. **Vinod PK, Sengupta N, Bhat PJ, Venkatesh KV.** 2008. Integration of global signaling pathways, cAMP-PKA, MAPK and TOR in the regulation of *FLO11*. PLoS One **3:**e1663. http://dx.doi.org/10.1371/journal.pone.0001663.
54. **Mösch HU, Fink GR.** 1997. Dissection of filamentous growth by transposon mutagenesis in *Saccharomyces cerevisiae*. Genetics **145:**671–684.
55. **Garí E, Volpe T, Wang H, Gallego C, Futcher B, Aldea M.** 2001. Whi3 binds the mRNA of the G1 cyclin CLN3 to modulate cell fate in budding yeast. Genes Dev **15:**2803–2808. http://dx.doi.org/10.1101/gad.203501.
56. **Wang H, Garí E, Vergés E, Gallego C, Aldea M.** 2004. Recruitment of Cdc28 by Whi3 restricts nuclear accumulation of the G1 cyclin-Cdk complex to late G1. EMBO J **23:**180–190. http://dx.doi.org/10.1038/sj.emboj.7600022.
57. **Schladebeck S, Mösch HU.** 2013. The RNA-binding protein Whi3 is a key regulator of developmental signaling and ploidy in *Saccharomyces cerevisiae*. Genetics **195:**73–86. http://dx.doi.org/10.1534/genetics.113.153775.
58. **Heise B, van der Felden J, Kern S, Malcher M, Brückner S, Mösch HU.** 2010. The TEA transcription factor Tec1 confers promoter-specific gene regulation by Ste12-dependent and -independent mechanisms. Eukaryot Cell **9:**514–531. http://dx.doi.org/10.1128/EC.00251-09.
59. **Brückner S, Kern S, Birke R, Saugar I, Ulrich HD, Mösch HU.** 2011. The TEA transcription factor Tec1 links TOR and MAPK pathways to coordinate yeast development. Genetics **189:**479–494. http://dx.doi.org/10.1534/genetics.111.133629.
60. **Van der Felden J, Weisser S, Brückner S, Lenz P, Mösch HU.** 2014. The transcription factors Tec1 and Ste12 interact with coregulators Msa1 and Msa2 to activate adhesion and multicellular development. Mol Cell Biol **34:**2283–2293. http://dx.doi.org/10.1128/MCB.01599-13.
61. **Yang X, Jiang R, Carlson M.** 1994. A family of proteins containing a conserved domain that mediates interaction with the yeast SNF1 protein kinase complex. EMBO J **13:**5878–5886.
62. **Jiang R, Carlson M.** 1997. The Snf1 protein kinase and its activating subunit, Snf4, interact with distinct domains of the Sip1/Sip2/Gal83 component in the kinase complex. Mol Cell Biol **17:**2099–2106.
63. **Kuchin S, Vyas VK, Carlson M.** 2003. Role of the yeast Snf1 protein kinase in invasive growth. Biochem Soc Trans **31:**175–177.
64. **Hedbacker K, Carlson M.** 2008. SNF1/AMPK pathways in yeast. Front Biosci **13:**2408–2420. http://dx.doi.org/10.2741/2854.
65. **Cullen PJ, Sprague GF, Jr.** 2000. Glucose depletion causes haploid invasive growth in yeast. Proc Natl Acad Sci U S A **97:**13619–13624. http://dx.doi.org/10.1073/pnas.240345197.
66. **Cullen PJ, Sprague GF, Jr.** 2012. The regulation of filamentous growth in yeast. Genetics **190:**23–49. http://dx.doi.org/10.1534/genetics.111.127456.
67. **Reynolds TB, Fink GR.** 2001. Bakers' yeast, a model for fungal biofilm formation. Science **291:**878–881. http://dx.doi.org/10.1126/science.291.5505.878.
68. **Palecek SP, Parikh AS, Huh JH, Kron SJ.** 2002. Depression of *Saccharomyces cerevisiae* invasive growth on non-glucose carbon sources requires the Snf1 kinase. Mol Microbiol **45:**453–469. http://dx.doi.org/10.1046/j.1365-2958.2002.03024.x.
69. **Van de Velde S, Thevelein JM.** 2008. Cyclic AMP-protein kinase A and Snf1 signaling mechanisms underlie the superior potency of sucrose for induction of filamentation in *Saccharomyces cerevisiae*. Eukaryot Cell **7:**286–293. http://dx.doi.org/10.1128/EC.00276-07.
70. **Ozcan S, Johnston M.** 1999. Function and regulation of yeast hexose transporters. Microbiol Mol Biol Rev **63:**554–569.
71. **Greatrix BW, van Vuuren HJ.** 2006. Expression of the *HXT13*, *HXT15* and *HXT17* genes in *Saccharomyces cerevisiae* and stabilization of the *HXT1* gene transcript by sugar-induced osmotic stress. Curr Genet **49:**205–217. http://dx.doi.org/10.1007/s00294-005-0046-x.
72. **Bermejo C, Haerizadeh F, Sadoine MS, Chermak D, Frommer WB.** 2013. Differential regulation of glucose transport activity in yeast by specific cAMP signatures. Biochem J **452:**489–497. http://dx.doi.org/10.1042/BJ20121736.
73. **Rintala E, Wiebe MG, Tamminen A, Ruohonen L, Penttilä M.** 2008. Transcription of hexose transporters of *Saccharomyces cerevisiae* is affected by change in oxygen provision. BMC Microbiol **8:**53. http://dx.doi.org/10.1186/1471-2180-8-53.
74. **Lafuente MJ, Gancedo C, Jauniaux JC, Gancedo JM.** 2000. Mth1 receives the signal given by the glucose sensors Snf3 and Rgt2 in *Saccharomyces cerevisiae*. Mol Microbiol **35:**161–172. http://dx.doi.org/10.1046/j.1365-2958.2000.01688.x.
75. **Young ET, Dombek KM, Tachibana C, Ideker T.** 2003. Multiple pathways are co-regulated by the protein kinase Snf1 and the transcription factors Adr1 and Cat8. J Biol Chem **278:**26146–26158. http://dx.doi.org/10.1074/jbc.M301981200.
76. **Tachibana C, Yoo JY, Tagne JB, Kacherovsky N, Lee TI, Young ET.** 2005. Combined global localization analysis and transcriptome data identify genes that are directly coregulated by Adr1 and Cat8. Mol Cell Biol **25:**2138–2146. http://dx.doi.org/10.1128/MCB.25.6.2138-2146.2005.
77. **Tachibana C, Biddick R, Law GL, Young ET.** 2007. A poised initiation complex is activated by SNF1. J Biol Chem **282:**37308–37315. http://dx.doi.org/10.1074/jbc.M707363200.
78. **Biddick RK, Law GL, Young ET.** 2008. Adr1 and Cat8 mediate coacti-

vator recruitment and chromatin remodeling at glucose-regulated genes. PLoS One **3:**e1436. http://dx.doi.org/10.1371/journal.pone.0001436.
79. **Frederick DL, Tatchell K.** 1996. The *REG2* gene of *Saccharomyces cerevisiae* encodes a type 1 protein phosphatase-binding protein that functions with Reg1p and the Snf1protein kinase to regulate growth. Mol Cell Biol **16:**2922–2931.
80. **Haurie V, Perrot M, Mini T, Jenö P, Sagliocco F, Boucherie H.** 2001. The transcriptional activator Cat8p provides a major contribution to the reprogramming of carbon metabolism during the diauxic shift in *Saccharomyces cerevisiae*. J Biol Chem **276:**76–85. http://dx.doi.org/10.1074/jbc.M008752200.
81. **Castermans D, Somers I, Kriel J, Louwet W, Wera S, Versele M, Janssens V, Thevelein JM.** 2012. Glucose-induced posttranslational activation of protein phosphatases PP2A and PP1 in yeast. Cell Res **22:**1058–1077. http://dx.doi.org/10.1038/cr.2012.20.
82. **François JM, Thompson-Jaeger S, Skroch J, Zellenka U, Spevak W, Tatchell K.** 1992. *GAC1* may encode a regulatory subunit for protein phosphatase type 1 in *Saccharomyces cerevisiae*. EMBO J **11:**87–96.
83. **Nigavekar SS, Tan YS, Cannon JF.** 2002. Glc8 is a glucose-repressible activator of Glc7 protein phosphatase-1. Arch Biochem Biophys **404:**71–79. http://dx.doi.org/10.1016/S0003-9861(02)00231-X.
84. **Hahn S, Young ET.** 2011. Transcriptional regulation in *Saccharomyces cerevisiae*: transcription factor regulation and function, mechanisms of initiation, and roles of activators and coactivators. Genetics **189:**705–736. http://dx.doi.org/10.1534/genetics.111.127019.
85. **Blumberg H, Hartshorne TA, Young ET.** 1988. Regulation of expression and activity of the yeast transcription factor ADR1. Mol Cell Biol **8:**1868–1876.
86. **Sloan JS, Dombek KM, Young ET.** 1999. Post-translational regulation of Adr1 activity is mediated by its DNA binding domain. J Biol Chem **274:**37575–37582. http://dx.doi.org/10.1074/jbc.274.53.37575.
87. **Kacherovsky N, Tachibana C, Amos E, Fox D, III, Young ET.** 2008. Promoter binding by the Adr1 transcriptional activator may be regulated by phosphorylation in the DNA-binding region. PLoS One **3:**e3213. http://dx.doi.org/10.1371/journal.pone.0003213.
88. **Cherry JR, Johnson TR, Dollard C, Shuster JR, Denis CL.** 1989. Cyclic AMP-dependent protein kinase phosphorylates and inactivates the yeast transcriptional activator ADR1. Cell **56:**409–419. http://dx.doi.org/10.1016/0092-8674(89)90244-4.
89. **Cook WJ, Chase D, Audino DC, Denis CL.** 1994. Dissection of the ADR1 protein reveals multiple, functionally redundant activation domains interspersed with inhibitory regions: evidence for a repressor binding to the ADR1c region. Mol Cell Biol **14:**629–640.
90. **Ratnakumar S, Kacherovsky N, Arms E, Young ET.** 2009. Snf1 controls the activity of adr1 through dephosphorylation of Ser230. Genetics **182:**735–745. http://dx.doi.org/10.1534/genetics.109.103432.
91. **Parua PK, Ratnakumar S, Braun KA, Dombek KM, Arms E, Ryan PM, Young ET.** 2010. 14-3-3 (Bmh) proteins inhibit transcription activation by Adr1 through direct binding to its regulatory domain. Mol Cell Biol **30:**5273–5283. http://dx.doi.org/10.1128/MCB.00715-10.
92. **Vyas VK, Kuchin S, Berkey CD, Carlson M.** 2003. Snf1 kinases with different beta-subunit isoforms play distinct roles in regulating haploid invasive growth. Mol Cell Biol **23:**1341–1348. http://dx.doi.org/10.1128/MCB.23.4.1341-1348.2003.
93. **Ishigami M, Nakagawa Y, Hayakawa M, Iimura Y.** 2004. *FLO11* is essential for flor formation caused by the C-terminal deletion of *NRG1* in *Saccharomyces cerevisiae*. FEMS Microbiol Lett **237:**425–430. http://dx.doi.org/10.1016/j.femsle.2004.07.012.
94. **Lamb TM, Mitchell AP.** 2003. The transcription factor Rim101p governs ion tolerance and cell differentiation by direct repression of the regulatory genes *NRG1* and *SMP1* in *Saccharomyces cerevisiae*. Mol Cell Biol **23:**677–686. http://dx.doi.org/10.1128/MCB.23.2.677-686.2003.
95. **Barrales RR, Jimenez J, Ibeas JI.** 2008. Identification of novel activation mechanisms for *FLO11* regulation in *Saccharomyces cerevisiae*. Genetics **178:**145–156. http://dx.doi.org/10.1534/genetics.107.081315.
96. **Kleinschmidt M, Grundmann O, Blüthgen N, Mösch HU, Braus GH.** 2005. Transcriptional profiling of *Saccharomyces cerevisiae* cells under adhesion-inducing conditions. Mol Genet Genomics **273:**382–393. http://dx.doi.org/10.1007/s00438-005-1139-4.
97. **Hinnebusch AG.** 2005. Translational regulation of GCN4 and the general amino acid control of yeast. Annu Rev Microbiol **59:**407–450. http://dx.doi.org/10.1146/annurev.micro.59.031805.133833.
98. **Valerius O, Kleinschmidt M, Rachfall N, Schulze F, López Marín S, Hoppert M, Streckfuss-Bömeke K, Fischer C, Braus GH.** 2007. The *Saccharomyces* homolog of mammalian RACK1, Cpc2/Asc1p, is required for *FLO11*-dependent adhesive growth and dimorphism. Mol Cell Proteomics **6:**1968–1979. http://dx.doi.org/10.1074/mcp.M700184-MCP200.
99. **Zeller CE, Parnell SC, Dohlman HG.** 2007. The RACK1 ortholog Asc1 functions as a G-protein beta subunit coupled to glucose responsiveness in yeast. J Biol Chem **282:**25168–25176. http://dx.doi.org/10.1074/jbc.M702569200.
100. **Rachfall N, Schmitt K, Bandau S, Smolinski N, Ehrenreich A, Valerius O, Braus GH.** 2013. RACK1/Asc1p, a ribosomal node in cellular signaling. Mol Cell Proteomics **12:**87–105. http://dx.doi.org/10.1074/mcp.M112.017277.
101. **Rubenstein EM, Schmidt MC.** 2007. Mechanisms regulating the protein kinases of *Saccharomyces cerevisiae*. Eukaryot Cell **6:**571–583. http://dx.doi.org/10.1128/EC.00026-07.
102. **Longtine MS, Theesfeld CL, McMillan JN, Weaver E, Pringle JR, Lew DJ.** 2000. Septin-dependent assembly of a cell cycle-regulatory module in *Saccharomyces cerevisiae*. Mol Cell Biol **20:**4049–4061. http://dx.doi.org/10.1128/MCB.20.11.4049-4061.2000.
103. **Howell AS, Lew DJ.** 2012. Morphogenesis and the cell cycle. Genetics **190:**51–77. http://dx.doi.org/10.1534/genetics.111.128314.
104. **King K, Jin M, Lew D.** 2012. Roles of Hsl1p and Hsl7p in Swe1p degradation: beyond septin tethering. Eukaryot Cell **11:**1496–1502. http://dx.doi.org/10.1128/EC.00196-12.
105. **Lew DJ.** 2003. The morphogenesis checkpoint: how yeast cells watch their figures. Curr Opin Cell Biol **15:**648–653. http://dx.doi.org/10.1016/j.ceb.2003.09.001.
106. **King K, Kang H, Jin M, Lew DJ.** 2013. Feedback control of Swe1p degradation in the yeast morphogenesis checkpoint. Mol Biol Cell **24:**914–922. http://dx.doi.org/10.1091/mbc.E12-11-0812.
107. **La Valle R, Wittenberg C.** 2001. A role for the Swe1 checkpoint kinase during filamentous growth of *Saccharomyces cerevisiae*. Genetics **158:**549–562.
108. **Prusty R, Grisafi P, Fink GR.** 2004. The plant hormone indoleacetic acid induces invasive growth in *Saccharomyces cerevisiae*. Proc Natl Acad Sci U S A **101:**4153–4157. http://dx.doi.org/10.1073/pnas.0400659101.
109. **Stankunas K, Berger J, Ruse C, Sinclair DA, Randazzo F, Brock HW.** 1998. The enhancer of polycomb gene of Drosophila encodes a chromatin protein conserved in yeast and mammals. Development **125:**4055–4066.
110. **Dohmen RJ, Willers I, Marques AJ.** 2007. Biting the hand that feeds: Rpn4-dependent feedback regulation of proteasome function. Biochim Biophys Acta **1773:**1599–1604. http://dx.doi.org/10.1016/j.bbamcr.2007.05.015.
111. **Owsianik G, Balzi l L, Ghislain M.** 2002. Control of 26S proteasome expression by transcription factors regulating multidrug resistance in *Saccharomyces cerevisiae*. Mol Microbiol **43:**1295–1308. http://dx.doi.org/10.1046/j.1365-2958.2002.02823.x.
112. **Bumgarner SL, Dowell RD, Grisafi P, Gifford DK, Fink GR.** 2009. Toggle involving *cis*-interfering noncoding RNAs controls variegated gene expression in yeast. Proc Natl Acad Sci U S A **106:**18321–18326. http://dx.doi.org/10.1073/pnas.0909641106.
113. **Halme A, Bumgarner S, Styles C, Fink GR.** 2004. Genetic and epigenetic regulation of the *FLO* gene family generates cell-surface variation in yeast. Cell **116:**405–415. http://dx.doi.org/10.1016/S0092-8674(04)00118-7.
114. **Herskowitz I.** 1988. Life cycle of the budding yeast *Saccharomyces cerevisiae*. Microbiol Rev **52:**536–553.
115. **Cappellaro C, Baldermann C, Rachel R, Tanner W.** 1994. Mating type-specific cell-cell recognition of *Saccharomyces cerevisiae*: cell wall attachment and active sites of a- and alpha-agglutinin. EMBO J **13:**4737–4744.
116. **Roberts CJ, Nelson B, Marton MJ, Stoughton R, Meyer MR, Bennett HA, He YD, Dai H, Walker WL, Hughes TR, Tyers M, Boone C, Friend SH.** 2000. Signaling and circuitry of multiple MAPK pathways revealed by a matrix of global gene expression profiles. Science **287:**873–880. http://dx.doi.org/10.1126/science.287.5454.873.
117. **Grote E.** 2008. Cell fusion assays for yeast mating pairs. Methods Mol Biol **475:**165–196. http://dx.doi.org/10.1007/978-1-59745-250-2_10.
118. **Merlini L, Dudin O, Martin SG.** 2013. Mate and fuse: how yeast cells do it. Open Biol **3:**130008. http://dx.doi.org/10.1098/rsob.130008.

119. **Suzuki K**. 2003. Roles of sexual cell agglutination in yeast mass mating. Genes Genet Syst **78:**211–219. http://dx.doi.org/10.1266/ggs.78.211.
120. **Willaert R**. 2010. Engineering aspects of cell immobilization. In Flickinger MC (ed), Encyclopedia of industrial biotechnology. John Wiley & Sons, Somerset, NJ.
121. **Granek JA, Kayıkçı Ö, Magwene PM**. 2011. Pleiotropic signaling pathways orchestrate yeast development. Curr Opin Microbiol **14:**676–681. http://dx.doi.org/10.1016/j.mib.2011.09.004.
122. **Neiman AM**. 2011. Sporulation in the budding yeast *Saccharomyces cerevisiae*. Genetics **189:**737–765. http://dx.doi.org/10.1534/genetics.111.127126.
123. **Šťovíček V, Váchová L, Palková Z**. 2012. Yeast biofilm colony as an orchestrated multicellular organism. Commun Integr Biol **5:**203–205. http://dx.doi.org/10.4161/cib.18912.
124. **Kuthan M, Devaux F, Janderová B, Slaninová I, Jacq C, Palková Z**. 2003. Domestication of wild *Saccharomyces cerevisiae* is accompanied by changes in gene expression and colony morphology. Mol Microbiol **47:**745–754. http://dx.doi.org/10.1046/j.1365-2958.2003.03332.x.
125. **Torbensen R, Møller HD, Gresham D, Alizadeh S, Ochmann D, Boles E, Regenberg B**. 2012. Amino acid transporter genes are essential for *FLO11*-dependent and *FLO11*-independent biofilm formation and invasive growth in *Saccharomyces cerevisiae*. PLoS One **7:**e41272. http://dx.doi.org/10.1371/journal.pone.0041272.
126. **Ielasi FS, Goyal P, Sleutel M, Wohlkonig A, Willaert RG**. 2013. The mannose-specific lectin domains of Flo1p from *Saccharomyces cerevisiae* and Lg-Flo1p from *S. Pastorianus*: crystallization and preliminary X-ray diffraction analysis of the adhesin-carbohydrate complexes. Acta Crystallogr Sect F Struct Biol Cryst Commun **69:**779–782. http://dx.doi.org/10.1107/S1744309113015030.
127. **Smyth GK**. 2004. Linear models and empirical bayes methods for assessing differential expression in microarray experiments. Stat Appl Genet Mol Biol **3:**Article3. http://dx.doi.org/10.2202/1544-6115.1027.
128. **Väremo L, Nielsen J, Nookaew I**. 2013. Enriching the gene set analysis of genome-wide data by incorporating directionality of gene expression and combining statistical hypotheses and methods. Nucleic Acids Res **41:**4378–4391. http://dx.doi.org/10.1093/nar/gkt111.
129. **Franceschini A, Szklarczyk D, Frankild S, Kuhn M, Simonovic M, Roth A, Lin J, Minguez P, Bork P, von Mering C, Jensen LJ**. 2013. String v9.1: protein-protein interaction networks, with increased coverage and integration. Nucleic Acids Res **41:**D808–D815. http://dx.doi.org/10.1093/nar/gks1094.
130. **Edgar R, Domrachev M, Lash AE**. 2002. Gene expression omnibus: NCBI gene expression and hybridization array data repository. Nucleic Acids Res **30:**207–210. http://dx.doi.org/10.1093/nar/30.1.207.
131. **Vaguine AA, Richelle J, Wodak SJ**. 1999. SFCHECK: a unified set of procedures for evaluating the quality of macromolecular structure-factor data and their agreement with the atomic model. Acta Crystallogr D Biol Crystallogr **55:**191–205. http://dx.doi.org/10.1107/S0907444998006684.